UNIVERSITY OF CALGARY

Quantum Process Tomography with Coherent States

by

Saleh Rahimi Keshari

A THESIS

SUBMITTED TO THE FACULTY OF GRADUATE STUDIES

IN PARTIAL FULFILLMENT OF THE REQUIREMENTS FOR THE

DEGREE OF MASTER OF SCIENCE

DEPARTMENT OF PHYSICS AND ASTRONOMY

AND

INSTITUTE FOR QUANTUM INFORMATION SCIENCE

CALGARY, ALBERTA

December, 2010

UNIVERSITY OF CALGARY

FACULTY OF GRADUATE STUDIES

The undersigned certify that they have read, and recommend to the Faculty of Graduate Studies for acceptance, a thesis entitled "Quantum Process Tomography with Coherent States" submitted by Saleh Rahimi Keshari in partial fulfillment of the requirements for the degree of MASTER OF SCIENCE.

Supervisor, Dr. Barry Sanders
Department of Physics and Astronomy

Co-supervisor, Dr. Alex Lvovsky
Department of Physics and Astronomy

Dr. Christoph Simon
Department of Physics and Astronomy

Dr. John R. Collins
Department of Mathematics and Statistics

Dr. Clifton Cunningham
Department of Mathematics and Statistics

NOV-30-2010
Date

Abstract

In this study, we develop an enhanced technique for characterizing quantum optical processes based on probing unknown quantum processes only with coherent states. Our method substantially improves the previous coherent-state quantum process tomography scheme in that it naturally circumvents the need for the Glauber-Sudarshan representation for states and the incurred P-function regularization used in the former scheme. This technique relies on a new relation between the action of a general quantum process on coherent state inputs and its action on an arbitrary quantum state. This relation not only introduces a substantial simplification in the process identification task but also naturally eliminates a potential source of estimation error associated with the P-function regularization. The new relation also enables straightforward extensions of coherent-state quantum process tomography to multi-mode and non-trace-preserving processes. We illustrate our formalism with several examples, in which we derive analytic representations of several fundamental quantum optical processes in the Fock basis. In particular, we introduce photon-number cutoff as a reasonable physical resource limitation and address resource-vs-accuracy trade-off in practical applications. We show that the accuracy of process estimation scales inversely with the square root of photon-number cutoff.

Acknowledgements

I would like to thank my supervisor, Dr. Barry Sanders, who has supported me throughout this project with his expertise, knowledge, and guidance. I also would like to thank my co-supervisor, Dr. Alex Lvovsky, for all helpful discussions, suggestions, and encouragements he gave me.

I would like to thank Dr. Artur Scherer for the time he devoted on this project, sharing his knowledge with me, conducting many useful discussions, and giving guidance on editing of my thesis. I am grateful to Dr. Ady Mann for his kind advice, helpful discussions, and for checking and correcting my calculations at the early stage of this project. I also would like to thank Dr. Ali Rezakhani for the helpful discussions and suggestions that he gave me during this project.

This work has been supported by Quantum Works, Alberta Innovates Technology Futures (AITF) and Pacific Institute for the Mathematical Sciences (PIMS).

Dedicated to:

My parents

Table of Contents

List of Tables

List of Figures

Glossary

$\mathcal{E}$	Quantum Process
$\mathcal{I}$	Identity Operator
AAPT	Ancilla-Assisted Process Tomography
BS	Beam Splitter
csQPT	coherent state Quantum Process Tomography
DCQD	Direct Characterization of Quantum Dynamics
PDC	Parametric Down-Conversion
POVM	Positive Operator Valued Measure
QPT	Quantum Process Tomography
QST	Quantum State Tomography
SQPT	Standard Quantum Process Tomography

Chapter 1

Introduction

The problem of characterizing quantum dynamics is of fundamental interest in the fields of quantum physics and quantum information science [1, 2]. For many practical applications, such as assembling a complex quantum information processor, we require precise knowledge of the properties of each component, i.e., the ability to predict the effect of the quantum devices on an arbitrary input state and characterize the underlying processes within quantum components. This gives rise to a quantum version of the famous "black-box problem", which is addressed by means of *quantum process tomography* (QPT) [4, 5]. Quantum process tomography has many applications ranging from probing of quantum communication channels to evaluation of the performance of quantum gates [4, 5, 6, 7, 8, 9, 10, 11].

Quantum information processing with optical systems is one of the most promising approaches to a fully-functional quantum computer [12]. Also, as the photons are excellent carriers of quantum information due to weak coupling to the environment implying low decoherence, and high speed, quantum optical systems are the obvious choice for quantum communication.

The aim of this thesis is to elaborate on QPT for quantum optical systems. In particular, we developed a new technique for characterizing quantum optical processes, which is a substantial improvement upon an existing method [13]. The main results presented in this thesis have been submitted for publication [14].

In some parts of this thesis, I quote verbatim from Ref. [14], which was written as a joint effort of the coauthors and I. In the next section we begin with describing quantum states and processes. In Sec. 1.2, quantum-state tomography is introduced as one of the tools for QPT. In particular, we describe the balanced homodyne detection as a device for quantum-optical state

tomography. QPT is reviewed in Sec. 1.3. The original proposal [13] for characterization of quantum-optical processes and the problems inherent to this approach are discussed in Sec. 1.4. The last section is an overview of this thesis. We briefly discuss how the problems of the original method are overcome by our new approach to quantum-optical process tomography.

1.1 Quantum states and processes

In quantum information processing, information is encoded into the state of quantum systems and processed by quantum operations. In this section we investigate the general mathematical properties of these two basic elements.

1.1.1 Quantum states

A quantum state is a mathematical object that embodies all information about the preparation of a quantum system [1]. Knowing the quantum state enables us to predict the probabilities of the outcomes for any measurements.

The most general formulation of measurements in quantum mechanics is POVM (Positive Operator Valued Measure) formalism [1]. A POVM is a set of operators $\{E_m\}$ on a Hilbert space such that each operator is positive semidefinite, and they sum to unity $\sum_m E_m = I$. The index m refers to an outcome of the measurement that take place in the experiment. If the system is prepared in state ρ, the probability for outcome m is given by

$$p(m) = \mathrm{Tr}[E_m \rho]. \tag{1.1}$$

This relation is known as Born's rule.

1.1.2 Quantum processes

The formalism of the quantum processes (also called quantum operations or quantum channels) provides a general framework for describing the evolution of quantum states in a wide

variety of circumstances [1, 15]. Assuming that the environment is independent of the device that prepares the state ρ, the most general transformation of a quantum state ρ allowed by the laws of quantum mechanics is described by a quantum process $\mathcal{E}$. A quantum process describes the evolution of any input state ρ into an output state

$$\rho' = \mathcal{E}(\rho). \tag{1.2}$$

A simple examples of quantum process is a unitary transformation $\mathcal{E}(\rho) = U\rho U^{\dagger}$. The quantum process formalism describes the dynamical changes that a quantum system undergoes as the result of some physical processes. Here ρ is the initial state and $\mathcal{E}(\rho)$ is the final state after the process.

The dynamics of a closed quantum system can be described by a unitary transformation. As in a real world, there are no perfectly isolated quantum systems, a real system always suffers from unwanted interactions with outside world, which lead to decoherence, losses. Thus, typically the quantum state ρ becomes entangled with the environment and the evolution of ρ cannot be described as a unitary transformation.

1.2 Quantum state tomography

In classical mechanics, the state of a system is described by a set of canonical coordinates; in principle it is always possible to set up an experiment consisting of multiple measurements by which the state can be fully recovered. In contrast, in quantum mechanics it is not possible to determine the state of a quantum system due to the limitations associated with the Heisenberg uncertainty principle [16, 17] and the no-cloning theorem [18]. On the one hand, one cannot perform an arbitrary sequence of measurements on a quantum system without disturbing it. On the other hand, it is not possible to make a perfect copy of quantum system without having complete knowledge about the system. Hence, if the quantum state of a system is unknown, there is no way to reconstruct the quantum state unless an ensemble of identically prepared

quantum systems is available [19].

Quantum-state tomography (QST) is a procedure for reconstructing the state of a quantum system ρ. In QST, by preparing many identical copies of a quantum system, one can perform a different measurement on each copy of the system and generate enough statistics to reconstruct the quantum state. In this procedure, the quantum state is fully recovered in the limit of large number of measurements. A set of observables for performing measurements on multiple copies of an unknown quantum system, which is sufficient for determination of the quantum state, is called a *quorum* [20]. QST is one of the tools for QPT and determining the output state of a quantum device. Also in quantum computing and information theory QST can be reliably used to determine the actual state of the qubits [1, 2].

QST is based on inverting Born's rule. The probabilities for d^2 ($d = \dim(\mathscr{H})$) independent outcomes obtained from the experiment specify a ρ_{tomo} consistent with these probabilities such that the estimation error is less than a given tolerance

$$\|\rho - \rho_{\text{tomo}}\|_1 < \delta, \tag{1.3}$$

where $\|\rho\|_1 = \text{Tr}\sqrt{\rho^\dagger \rho}$ is the trace norm. In QST, measurements must be repeated to yield *frequencies* from which the probabilities can be inferred. If the measurement is repeated N times, and outcome m is obtained n_m times, then the frequency is

$$f_m = \frac{n_m}{N}. \tag{1.4}$$

For sufficiently many of measurements, one can estimate the associated probability with the operator E_m

$$p(m) \approx f_m. \tag{1.5}$$

For the measurements that form a quorum, the equations

$$\text{Tr}[E_m \rho] = \frac{n_m}{N} \tag{1.6}$$

form a complete set of equations, which can be solved to obtain the estimated state ρ_{tomo} [21]. Therefore, a tomography method searches for a density matrix ρ_{tomo} on the space of semi-positive-definite hermitian operators describing physical states whose predictions be in agreement with the observed frequencies. There are several methods for quantum-state tomography; for a review of the methods see Ref. [2]. Unfortunately, some quantum tomography methods generate the estimated state ρ_{tomo} that does not satisfy the physical conditions for quantum states (see Sec. 2.1) [21]. For instance, ρ_{tomo} could have a negative eigenvalue, an eigenvalue greater than 1, or zero eigenvalues that cannot be justified by the data.

In the case of infinite-dimensional Hilbert space, no finite number of measurements constitute a quorum. Hence, certain assumptions about the structure of the state in question must be made to limit the number of free parameters. A finite measurement together with the assumptions lead to some errors in estimated states (1.3) [22].

1.2.1 Optical-homodyne tomography

In this subsection, we describe balanced homodyne detector as a device for tomography of the quantum state of light. In this case, we are dealing with a quantum system, which has an infinite-dimensional Hilbert space.

The Hamiltonian of the quantum system of light with frequency ω with certain polarization, referred to as single electromagnetic-field mode, is equivalent to that of a quantum particle in a one-dimensional harmonic potential,

$$\hat{H} = \omega(\hat{a}^\dagger \hat{a} + 1/2), \tag{1.7}$$

where $\hat{a}$ and $\hat{a}^\dagger$ are annihilation and creation operators of the electromagnetic-field mode, respectively[1], satisfying the commutator relation $[\hat{a}, \hat{a}^\dagger] = 1$. The operator $\hat{n} \equiv \hat{a}^\dagger \hat{a}$ is known as *photon-number* operator, its eigenvalues represent the number of photons. The eigenvalues of

[1] In this thesis, we consider $\hbar \equiv 1$.

this Hamiltonian are denoted by $h_n = (n+1/2)\omega$. They correspond to the energy levels of the system. The energy spectrum is quantized with equally-spaced energy levels. The eigenstates of $\hat{H}$, $\{|n\rangle\}$, are referred to as Fock states or photon-number states. They form a complete basis for the Hilbert space. The quantum state of a particle in a harmonic potential can be represented in the Fock basis or equivalently in terms of the function that describes position and momentum of the particle; hence, a quantum state of light can also be represented in terms of a similar function [25].

In quantum optics, the quadratures $\hat{q}$ and $\hat{p}$ are regarded as position and momentum operators of the electromagnetic oscillator. They satisfy the commutator relation $[\hat{q}, \hat{p}] = i$ and are defined as

$$\hat{q} = \frac{\hat{a}^\dagger + \hat{a}}{\sqrt{2}}, \tag{1.8}$$

$$\hat{p} = \frac{i(\hat{a}^\dagger - \hat{a})}{\sqrt{2}}. \tag{1.9}$$

In the balanced homodyne detection [23, 24], the signal field and a strong laser beam called local oscillator (LO) overlap at a 50% reflecting beam splitter. After the beam splitter, each beam is detected by a photodetector, and the photocurrents I_1 and I_2 are measured. The interference term of the LO and the signal is captured in the difference photocurrent $I_{12} \equiv I_2 - I_1$. The scheme of a balanced homodyne detector is shown in Fig. 1.1. For a single mode of the electromagnetic-field, by using balanced homodyne detection, one can measure the linear combinations of quadratures of a harmonic oscillator [25]

$$\begin{aligned} \hat{q}_\theta &= \hat{q}\cos\theta + \hat{p}\sin\theta \\ &= \frac{\hat{a}^\dagger e^{i\theta} + \hat{a}e^{-i\theta}}{2}, \end{aligned} \tag{1.10}$$

where the phase reference θ for the quadrature measurement is provided by the LO. The phase θ can be varied by adjusting the LO using, for instance, a piezo-electrically movable mirror

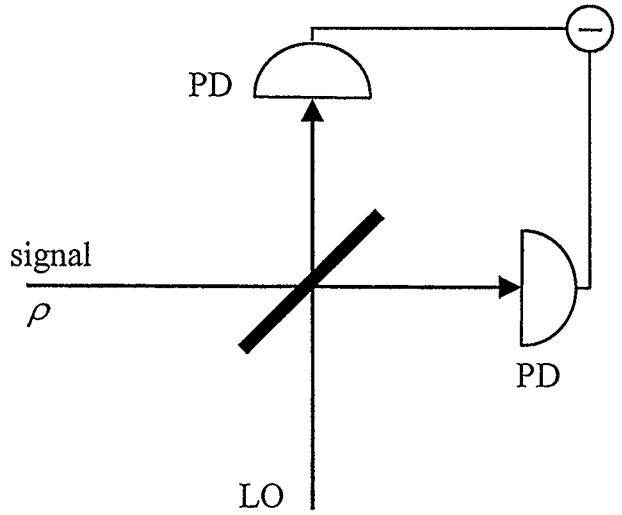

Figure 1.1: Scheme of the balanced homodyne detector. PD denotes the photodetector. The signal overlaps with the LO on a 50% beam splitter, and the outputs are measured by the PDs. The minus sign indicates that the difference photocurrent is measured.

[25]. Hence, $\hat{q}_\theta$ can be measured for different phases, and a POVM is

$$E(q_\theta) \equiv |q_\theta\rangle\langle q_\theta|, \tag{1.11}$$

where $|q_\theta\rangle$ is an eigenstate of the quadrature $\hat{q}_\theta$ with eigenvalue q. Note that the POVMs are labeled by a continuous index q and θ rather than by a discrete index.

By using a balanced homodyne detector, the probabilities

$$p(q,\theta) = \mathrm{Tr}[|q_\theta\rangle\langle q_\theta|\rho], \tag{1.12}$$

can be estimated, and by employing a tomography method, the quantum-optical state can be reconstructed. There are various methods for reconstruction of a state using the data, such as inverse Radon transformation, maximum-likelihood or maximum-entropy; for a review of the methods see Ref. [22].

1.3 Quantum process tomography

Quantum process tomography (QPT) is a procedure for estimating an unknown quantum process. Process tomography is successful if, for every input state, the estimate for the process output closely approximates the process output state that can be reconstructed using quantum-state tomography techniques. The worst-case error of this estimate, given by a distance (1.3) between the reconstructed and estimated process outputs, is less than a given tolerance.

There are two types of methods for QPT: direct and indirect [3]. In indirect methods, the effects of unknown quantum process on a complete set of probe states are found via QST on the process output states, and the quantum process is characterized by applying an inversion map on the output data. These methods are called indirect since QST is required to characterize a quantum process. Standard Quantum Process Tomography (SQPT) [4, 5] and Ancilla-Assisted Process Tomography (AAPT) [9, 26, 27, 28] are in this class. On the other hand, in direct methods experimental outcomes directly provide information about a quantum process, without using QST. The method of Direct Characterization of Quantum Dynamics (DCQD) [29, 30] belongs to this class.

In SQPT, a quantum device can be characterized in the same way as for any classical linear system; the only difference is that, in the quantum case, one needs many copies of the output states to perform quantum tomography. SQPT exploits linearity of quantum process over its density operators. If the effect of the process $\mathcal{E}(\rho_i)$ is known for a set of density operators $\{\rho_i\}$, its effect on any linear combination $\rho = \sum_i \beta_i \rho_i$ equals $\mathcal{E}(\rho) = \sum_i \beta_i \mathcal{E}(\rho_i)$. Therefore, if $\{\rho_i\}$ forms a spanning set within the space $\mathscr{L}(\mathscr{H})$ of linear operators over a particular Hilbert space $\mathscr{H}$, knowledge of $\{\mathcal{E}(\rho_i)\}$ is sufficient to extract complete information about the quantum process. SQPT was achieved by this method in liquid-state nuclear magnetic resonance [31, 32, 33], atomic [34], solid-state [35], and quantum optical systems [36, 37].

However, practical implementations of SQPT become demanding especially for systems

with large Hilbert spaces. For $\dim(\mathscr{H}) = d$, $\dim\big(\mathscr{L}(\mathscr{H})\big) = d^2$, which implies that at least d^2 unknown operators $\{\mathcal{E}(\rho_i)\}$, each with d^2 unknown parameters, must be estimated. This procedure requires preparation of at least $\{\rho_i\}_{i=1}^{d^2}$ states, subjecting each to the unknown process $\mathcal{E}$, and determining each element of $\{\mathcal{E}(\rho_i)\}_{i=1}^{d^2}$ through measurement (each with d^2 unknown elements), thereby inferring an overall number of d^4 parameters. Furthermore, in order to build up sufficient statistics for reliable estimates of the output states, each measurement should be performed many times on multiple copies of the inputs. Thus, a large number of realizations and measurements are required for complete tomography of $\mathcal{E}$.

An additional complication, especially for SQPT of quantum *optical* processes, is associated with preparation of the probe states. Typical optical SQPT implementations deal with systems consisting of one or more dual-rail qubits [36, 37] with postselection based on photon coincidences projecting the input and output states onto these qubit subspaces. Due to optical losses, imperfect sources and detector dark counts the input and output states departure from the qubit subspace, and this approach cannot provide complete information about a process. Furthermore, the probe states are highly nonclassical, hence difficult to generate.

In AAPT, an ancilla system with Hilbert space dimension at least as great as that of the principal system is required. The process $\mathcal{E}$ is characterized by preparing the combined system in a single state, σ, such that all information about the process can be imprinted on the final state $(\mathcal{E} \otimes \mathcal{I})(\sigma)$ [9, 26]. By performing QST on the final state the required information for characterizing the quantum process can be extracted. In principle, the input state, σ, can be prepared in either entanglement-assisted or a separable mixed state. However, it has been shown that use of maximally entangled pure states offers the best performance [3].

In DCQD, similarly to AAPT, an ancilla system is required. DCQD is based on using certain entangled states as input and a certain set of error-detecting measurements [1]. A combination of these input states and measurements lead to direct encoding of the information about the quantum process into the measurement results, which eliminates the need for QST.

In quantum optics, the complication associated with implementation of AAPT schemes [26, 27] and DCQD [29, 30, 38] is the preparation of maximally- or highly-entangled probe states. In particular, for large-dimensional Hilbert space these probe states are difficult to prepare.

In all above mentioned methods for QPT (SQPT, AAPT, DCQD), quantum-optical process tomography is restricted to low-dimensional Hilbert spaces. Thus, a method with available probe states and applicable to arbitrarily large Hilbert spaces needs to be invoked.

1.4 Coherent-state quantum-process tomography

The difficulties for QPT have been partially alleviated in the recently-proposed scheme "coherent-state quantum-process tomography" (csQPT) [13], as a method for complete characterization of a general quantum-optical process. This scheme is based on probing unknown quantum optical processes by coherent states [39], which are classical fields produced by common laser sources.

The scheme of csQPT is based on the observation that the density operator ρ of a generic quantum state of every electromagnetic mode can be decomposed in terms of coherent states $|\alpha\rangle$ using the *Glauber-Sudarshan representation* [40, 41]:

$$\rho = \int_{\mathbb{C}} \mathrm{d}^2\alpha \, P_\rho(\alpha) |\alpha\rangle\langle\alpha|, \tag{1.13}$$

where $P_\rho(\alpha)$ is a quasi-probability distribution, as a representation for the state, referred to as the quantum state's "P-function" and integrated over the entire complex plane. α is a complex number with $\alpha = (q + ip)/\sqrt{2}$ and corresponds to a point in two-dimensional space, which is called *phase space*. Linearity of the quantum process hence implies that measuring

$$|\alpha\rangle\langle\alpha| \mapsto \varrho_{\mathcal{E}}(\alpha) \equiv \mathcal{E}(|\alpha\rangle\langle\alpha|), \tag{1.14}$$

i.e., determining the effect of the unknown process on *all* coherent states, enables a prediction

of its effect upon any generic state ρ according to

$$\mathcal{E}(\rho) = \int_{\mathbb{C}} \mathrm{d}^2\alpha \, P_\rho(\alpha) \varrho_\varepsilon(\alpha). \tag{1.15}$$

The implementation of csQPT is advantageous because (i) coherent states are readily available from lasers, (ii) coherent states of different amplitudes and phases can be produced without changing the layout of the experimental apparatus, and (iii) output-state characterization can be performed using optical homodyne tomography [22], which obviates the need for postselection and provides full information about the process in question. This method has been tested experimentally on simple single-mode processes, such as the identity, attenuation, and phase shift operations [13]. Furthermore, csQPT has been used to characterize quantum memory for light based on electromagnetically-induced transparency [42].

An apparent obstacle to csQPT, however, is that the Glauber-Sudarshan representation does not exist for many quantum optical states [43, 44]. For some states the P-function is an singular generalized function that is not compatible with the form of the Glauber-Sudarshan representation (see Sec. 2.4). Hence, in general, some "regularization" is needed [45, 46]. A remedy therefor is provided by Klauder's theorem [47], which states that any trace-class operator ρ (whose trace-norm is finite: $\|\rho\|_1 < \infty$) can be approximated, to arbitrary accuracy, by a bounded operator $\rho_L \in \mathscr{B}(\mathscr{H})$ whose Glauber-Sudarshan function P_L is in the Schwartz class [48], so integration Eq. (1.15) can be performed. The Klauder approximation can be constructed by low-pass filtering of the P function, i.e., by multiplying its Fourier transform with an appropriate regularizing function equal to 1 over a square domain of size $L \times L$ and rapidly dropping to zero outside this domain. Ref. [13] employs this method to implement csQPT. In this proposal, the formalism for characterizing a quantum-optical process in the Fock basis is based on using the regularization function and depends on cutoff parameter L.

Practical implementation of Klauder's procedure is however complicated, because it requires finding the characteristic function of the input state and subsequently its regularized P

function. This function features high-frequency, high-amplitude oscillations that limit the precision in calculating the output state (1.15). Furthermore, Klauder's approximation is ambiguous with regard to the choice of the particular filtering function as well as the cutoff parameter L [13]. Errors of using Klauder's approximation translates into errors in the process estimation and there is no known method to bound this error. These ambiguities can potentially limit applications of csQPT; hence, they need to be overcome.

1.5 This thesis

This thesis introduces a new, more efficient technique, which I have found, for quantum-optical process tomography in the Fock (photon-number) basis [14]. I improve the existing method for csQPT [13] by overcoming the problems associated with P-function regularization. Specifically, the new method eliminates the explicit use of the Glauber-Sudarshan representation and thus removes the inherent ambiguity associated with employing Klauder's approximation for csQPT. This elimination substantially simplifies csQPT and leads to some significant results, which are presented in this thesis.

This thesis is organized as follows:

Chapter 2 provides an overview of the mathematical tools for the new method of csQPT. First we introduce a representation for a quantum process, which is called "process tensor", and discuss symmetries and the multi-mode case. In Sec. 2.3, we discuss how QPT can be performed for quantum states defined over infinite-dimensional Hilbert space by restricting to a finite-dimensional subspace using a regularization operator. We present a method for calculating the error associated with this restriction for energy non-increasing processes. Furthermore, we review the Glauber-Sudarshan representation in more detail and its existence condition in Sec. 2.4.

In Chapter 3, we introduce our new csQPT technique. We obtain an expression for the

process tensor in the Fock basis that can be calculated from the experimental data. Using this tensor, the process output for an arbitrary input can be calculated by simple matrix multiplication. In this way, transformations between the Fock and Glauber-Sudarshan representations, which were necessary in Ref. [13], can be sidestepped. Using our new approach, we easily extend csQPT from its restrictive single-mode applicability to multi-mode processes and even to non-trace-preserving conditional processes. These extensions are particularly relevant for quantum information processing circuits, whose basic components are inherently multi-mode and conditional [49]. Moreover, in Sec. 3.2, we illustrate our method by analytically deriving the process tensor for certain fundamental quantum optical processes using the Fock basis.

In Chapter 4, the practical application of the method is investigated for the case of phase-symmetric processes, which are realized in many practical situations; that is, an optical phase shift of the input state results in the same phase shift of the output. This property dramatically simplifies the experiment because one just needs to find the effects of the process on discrete set of coherent states with the same phase. This prompts us to discuss, in Sec. 4.2, how to obtain the process tensor for phase-symmetric processes. Furthermore, we discuss the error analysis of our new method, and compare the sources of errors in the method with those of the original proposal [13].

Chapter 5 summarizes the advantages of our new method and concludes. We wrap up in the last chapter by suggesting future work based on our method.

Chapter 2

Toolbox

In this chapter, we introduce the mathematical tools required to describe our new method for csQPT. In Sec. 2.1, we introduce a representation for a quantum state. In Sec. 2.2, we consider a representation for a quantum process and discuss the symmetry of the process and the multi-mode case. In Sec. 2.3, we discuss QPT for states over infinite-dimensional Hilbert spaces. We show that by employing a regularization operator restricting to a finite-dimensional subspace of the Hilbert space, QPT can be done with finite sampling. Moreover, we show that the error in the process estimation scales inversely with the square root of photon-number cutoff.

The Gluaber-Sudarshan representation plays the main role in csQPT. In Sec. 2.4, we examine The Gluaber-Sudarshan representation and the existence condition of the representation in closer detail.

The calculation of the error in the process estimation, which is presented in Subces. 2.3.1, is one of my project results in collaboration with the coauthors of Ref. [14]. I quote this subsection verbatim.

2.1 Representation of a quantum state

In quantum physics, a quantum state can be pure or mixed. If the state is pure, it can be represented by a normalized vector $|\psi\rangle$ in the Hilbert space associated with that system. A mixed state can always be represented as a statistical mixture of pure states.

A convenient way for describing quantum systems is the density operator language [1]. In general, suppose a quantum system is in one of the states $\{|\psi_i\rangle\}$, with respective probabilities

$\{p_i\}$. We call $\{p_i, |\psi_i\rangle\}$ an *ensemble of pure states*, and the density operator for the system is defined as

$$\rho \equiv \sum_i p_i |\psi_i\rangle\langle\psi_i|. \tag{2.1}$$

The density operator ρ has the following properties:

- ρ has trace equal to one, $\mathrm{Tr}[\rho] = 1$,
- ρ is Hermitian,
- eigenvalues p_i of ρ are nonnegative.

A quantum state ρ belongs to $\mathscr{B}(\mathscr{H})$, denoting the set of all linear bounded operators acting on the Hilbert space $\mathscr{H}$.

Let $\{|\varphi_n\rangle\}_{n=0}^{d-1}$ be an orthonormal basis for the Hilbert space $\mathscr{H}$ with dimension d. Then any state ρ can be represented as

$$\rho = \sum_{n,m=0}^{d-1} \rho_{nm} |\varphi_n\rangle\langle\varphi_m|, \tag{2.2}$$

where $\rho_{nm} = \langle\varphi_n|\rho|\varphi_m\rangle$ is the matrix representation of the density operator referred to as the *density matrix*.

2.2 Representation of a quantum process

A mapping $\mathcal{E}$ over the space of all bounded operators $\mathscr{B}(\mathscr{H})$ is a quantum process if it satisfies the following conditions [1]:

- $\mathcal{E}$ is linear: $\mathcal{E}(\rho_1 + \rho_2) = \mathcal{E}(\rho_1) + \mathcal{E}(\rho_2)$.
- $\mathcal{E}$ is trace non-increasing: $\mathrm{Tr}[\mathcal{E}(\rho)] \leq \mathrm{Tr}[\rho]$.
- $\mathcal{E}$ is completely positive, i.e., for any auxiliary Hilbert space $\mathscr{H}_a$, $\sigma \geq 0$ in $\mathscr{B}(\mathscr{H} \otimes \mathscr{H}_a)$ implies $(\mathcal{E} \otimes \mathcal{I}_a)(\sigma) \geq 0$ where $\mathcal{I}_a$ is the identity operation on $\mathscr{B}(\mathscr{H}_a)$.

There are several ways to describe a quantum process mathematically [1]. A widely-used formalism to describe a quantum process is the *Kraus decomposition* [15]. In this description, every quantum process can be expressed as

$$\mathcal{E}(\rho) = \sum_i \hat{K}_i \rho \hat{K}_i^\dagger, \tag{2.3}$$

where $\{\hat{K}_i\}$ are Kraus operators on the system's Hilbert space. It can be shown that $\sum_i \hat{K}_i^\dagger \hat{K}_i = \mathcal{I}$ for trace-preserving processes, and in general $\sum_i \hat{K}_i^\dagger \hat{K}_i \leq \mathcal{I}$ for non-trace-preserving processes, in order to guarantee $\mathrm{Tr}[\mathcal{E}(\rho)] \leq 1$.

In what follows, we provide a representation for a quantum process considering the basis $\{|\varphi_n\rangle\}$ for the Hilbert space. By subjecting a quantum state ρ to the quantum process $\mathcal{E}$, and exploiting linearity, from Eq. (2.2) we obtain

$$\mathcal{E}(\rho) = \sum_{n,m=0}^{d-1} \rho_{nm} \mathcal{E}(|\varphi_n\rangle\langle\varphi_m|). \tag{2.4}$$

From this equation, the matrix elements of the input and output states are related by

$$[\mathcal{E}(\rho)]_{jk} = \sum_{n,m=0}^{d-1} \mathcal{E}_{jk}^{nm} \rho_{nm}, \tag{2.5}$$

where

$$\mathcal{E}_{jk}^{nm} = \langle\varphi_j|\mathcal{E}(|\varphi_n\rangle\langle\varphi_m|)|\varphi_k\rangle \tag{2.6}$$

is a rank-4 tensor, hereafter referred to as the "process tensor" or the "superoperator". By using the process tensor the output state of the quantum process is given by

$$\mathcal{E}(\rho) = \sum_{n,m,j,k=0}^{d-1} \mathcal{E}_{jk}^{nm} \rho_{nm} |\varphi_j\rangle\langle\varphi_k|. \tag{2.7}$$

Thus, a quantum process can be represented by the process tensor by which the output state can be found for any given input state. Estimating all d^4 elements of the process tensor is the ultimate goal of quantum process tomography.

2.2.1 Symmetry

For many practical application of QPT, we may have partial knowledge, such as symmetry information, about the quantum process in question. This information may be known prior to process tomography or be obtained through an experiment. Having symmetry information about a quantum process reduces the number of unknown elements in the process tensor.

For example, if trace of quantum states are preserved under the quantum process, then from Eq. (2.5) we obtain

$$\sum_{j=0}^{d-1}[\mathcal{E}(\rho)]_{jj} = \sum_{j,n,m=0}^{d-1} \mathcal{E}_{jj}^{nm}\rho_{nm} = 1. \tag{2.8}$$

For d^2 independent density matrices over the Hilbert space with dimension d, Eq. (2.8) leads to d^2 constraints that reduce the number of unknown elements in the process tensor to $d^4 - d^2$.

As another example, suppose that the basis $\{|\varphi_i\rangle\}$ vectors are eigenvectors of a Hermitian operator A

$$A|\varphi_i\rangle = a_i|\varphi_i\rangle. \tag{2.9}$$

If the quantum process is symmetric with respect to the operator A, i.e.,

$$\mathcal{E}(A\rho A^\dagger) = A\mathcal{E}(\rho)A^\dagger, \tag{2.10}$$

then from Eq. (2.6) we have

$$\langle\varphi_j|\mathcal{E}(A|\varphi_n\rangle\langle\varphi_m|A^\dagger)|\varphi_k\rangle = \langle\varphi_j|A\mathcal{E}(|\varphi_n\rangle\langle\varphi_m|)A^\dagger|\varphi_k\rangle. \tag{2.11}$$

This equation yields

$$a_n\bar{a}_m = a_j\bar{a}_k. \tag{2.12}$$

Therefore, using Eq. (2.12) one of the parameters in the process tensor can be written in terms of others and the number of unknown elements reduces to d^3.

2.2.2 Multi-mode process

A multi-mode quantum process is a mapping over the density matrices defined over the Hilbert space that is tensor product of Hilbert spaces for individual modes. In the M-mode case, the Hilbert space is $\mathscr{H} = \mathscr{H}_1 \otimes \mathscr{H}_2 \otimes \cdots \otimes \mathscr{H}_M$, where each Hilbert space is associated with a different mode of oscillation.

Let us consider a representation for a multi-mode process. For the M-mode Hilbert space we use the notation

$$|\varphi_n\rangle := |\varphi_{n_1}, \varphi_{n_2}, \ldots, \varphi_{n_M}\rangle \tag{2.13}$$

with $n \in \mathbb{N}_0^M$, where $\mathbb{N}_0 \equiv \mathbb{N} \cup \{0\}$. Then a density matrix can be expressed as

$$\rho = \sum_{n,m \in \mathbb{N}_0^M} \rho_{nm} |\varphi_n\rangle\langle\varphi_m|. \tag{2.14}$$

From a similar procedure to the single-mode case, we find that the matrix elements of the input and output states are related by

$$[\mathcal{E}(\rho)]_{jk} = \sum_{n,m \in \mathbb{N}_0^M} \mathcal{E}_{jk}^{mn} \rho_{nm}, \tag{2.15}$$

where

$$\mathcal{E}_{jk}^{nm} := \langle\varphi_j|\mathcal{E}(|\varphi_n\rangle\langle\varphi_m|)|\varphi_k\rangle \tag{2.16}$$

is the rank-4^M tensor that is the M-mode process tensor representing the process.

2.3 Regularization

As the number of linearly independent probe states required for QPT must be at least $(\dim(\mathscr{H}))^2$, for states over an infinite-dimensional Hilbert space, such as optical state, the finiteness of resources and sampling implies that the process is necessarily under-sampled. However, process tomography is regarded to be successful (see Sec. 1.2) if the predicted output state, by using the estimated process $\mathcal{E}_{\text{tomo}}$, is a close approximation of the measured output

state using QST. In this section, we show that by employing an appropriate regularization operator that restricts the space of tomography to a finite-dimensional *subset* of $\mathscr{B}(\mathscr{H})$, the problem of under-sampling can be avoided. This reduced process tomography can always be successful with a sufficiently large amount of sampling.

To clarify the issue, let us consider the ideal case. Suppose that Alice prepares and send a quantum state through a quantum process (e.g. a quantum channel) to Bob. We assume that Bob has an ideal measurement device associated with POVM E_m and access to the entire Hilbert space (infinite recourses). In this case, if the process is trace-preserving, the probability of the measurement outcome m that Bob observes is given by

$$p(m) = \mathrm{Tr}[E_m \mathcal{E}(\rho)] = \sum_{j,k=0}^{\infty} [E_m]_{jk} [\mathcal{E}(\rho)]_{jk}, \tag{2.17}$$

where $[E_m]_{kj}$ is the matrix element of the POVM element associated with the outcome m. On the contrary, in a real world, due to the finiteness of recourses the probability that Bob estimates for the outcome m, by performing the experiment many times, is $p_{\mathrm{est}}(m)$. In general, this probability might be different from the ideal value $p(m)$. Therefore, the information that Bob can extract from the output state is always restricted and depends on the measurement device.

Now, if we employ a regularization operator K_N in Eq. (2.17), which restricts the space to a finite-dimensional subspace of the Hilbert space, then we obtain

$$p_{\mathrm{reg}}(m) = \mathrm{Tr}[E_m K_N \mathcal{E}(\rho) K_N^\dagger] = \sum_{i,l,j,k,=0}^{\infty} [E_m]_{il} [K_N]_{lj} [\mathcal{E}(\rho)]_{jk} [K_N^\dagger]_{ki}, \tag{2.18}$$

where $p_{\mathrm{reg}}(m)$ is the probability of observing outcome m from the state $K_N \mathcal{E}(\rho) K_N^\dagger$ in the finite subspace. N is the parameter of the regularization, which defines the dimension of the truncated Hilbert space. Therefore, if there exists K_N such that the difference between $p_{\mathrm{reg}}(m)$ and $p_{\mathrm{est}}(m)$ be small, i.e. $|p_{\mathrm{est}}(m) - p_{\mathrm{reg}}(m)| \ll 1$, then QPT can be restricted to a finite-dimensional subset of $\mathscr{B}(\mathscr{H})$ defined by the regularization operator K_N, so process tomography can successfully be performed with a sufficiently large finite sampling.

The general form that we can consider for the regularization operator in the Fock basis is

$$K_N = \sum_{n=0}^{\infty} f_N(n)|n\rangle\langle n|. \tag{2.19}$$

The accuracy of regularization depends on the form of the operator $f_N(n)$. For example, the regularization operator can be the projection operator onto the subspace $\widetilde{\mathscr{H}}$ with the dimension $N+1$

$$K_N = \widetilde{\Pi}_N \equiv \sum_{n=0}^{\infty} H[N-n]|n\rangle\langle n|, \tag{2.20}$$

where $H[n]$ is the discrete case of the unit step function. In the next section, by using this projection operator, we provide process error estimate when the space of tomography is restricted to $\mathscr{B}(\widetilde{\mathscr{H}})$.

2.3.1 Energy cutoff and estimation of the error of approximation

Here we focus on QPT in quantum optics. The state space is the Fock space which is an infinite-dimensional Hilbert space associated with a single-mode electromagnetic field [14].

Of particular practical interest is the subspace $\mathcal{B}(\tilde{\mathcal{H}})$ defined by an energy cut-off, i.e., estimating the process without accessing any information about its high-energy behavior. This restriction is naturally consistent with our choice to work in the Fock basis, because then the resulting process tensor is of finite size, and with many practical settings (e.g. quantum-information processing with photonic qubits).

The incompleteness of the information acquired in the experiment is accommodated in QPT by evaluating the process tensor over a restricted finite-dimensional subspace $\widetilde{\mathscr{H}}$ of the Hilbert space $\mathscr{H}$ with a fixed maximum number N of photons. The incurred expense is that, through this reduced tomography, only approximate information about the process will be inferred: for a given input state ρ, the predicted output is not $\mathcal{E}(\rho)$, but rather $\tilde{\mathcal{E}}(\tilde{\rho})$, where

$$\tilde{\rho} = \frac{\widetilde{\Pi}_N \rho \widetilde{\Pi}_N}{\mathrm{Tr}[\rho \widetilde{\Pi}_N]} \tag{2.21}$$

is the trace-normalized projection of ρ onto $\mathscr{B}(\widetilde{\mathscr{H}})$ and

$$\tilde{\mathcal{E}}(\tilde{\rho}) = \widetilde{\Pi}_N \mathcal{E}(\tilde{\rho}) \widetilde{\Pi}_N \tag{2.22}$$

is the predicted output of the reconstructed process for input state $\tilde{\rho}$. In Eqs. (2.21) and (2.22), $\widetilde{\Pi}_N$ is defined in Eq. (2.20).

If the input state ρ is outside $\mathscr{B}(\widetilde{\mathscr{H}})$, the process output estimation error $\|\mathcal{E}(\rho) - \tilde{\mathcal{E}}(\tilde{\rho})\|_1$ is generally unbounded. However, it is possible to bound the error for certain practically important classes of input states and processes.

For example, all linear-optical processes involving only linear-optical elements (interferometers, attenuators, conditional measurements) do not generate additional photons, and thus map $\mathscr{B}(\widetilde{\mathscr{H}})$ onto itself, so $\tilde{\mathcal{E}}(\tilde{\rho}) = \mathcal{E}(\tilde{\rho})$. For such processes, the error for a particular input ρ can be estimated according to $\|\mathcal{E}(\rho) - \mathcal{E}(\widetilde{\rho})\|_1 \leq \|\mathcal{E}\| \, \|\rho - \widetilde{\rho}\|_1$, with the superoperator norm defined as $\|\mathcal{E}\| \equiv \sup\{\|\mathcal{E}(\hat{B})\|_1 \, : \, \hat{B} \in \mathscr{B}(\mathscr{H}) \, , \, \|\hat{B}\|_1 \leq 1\}$ [50]. If the process is known to be non-trace-increasing, we have $\|\mathcal{E}\| \leq 1$ [1] so the error is bounded from above by

$$\|\mathcal{E}(\rho) - \mathcal{E}(\widetilde{\rho})\|_1 \leq \|\rho - \widetilde{\rho}\|_1. \tag{2.23}$$

Note that the above result is not sufficient for evaluating the error for a general process, because this error is given by the deviation of $\mathcal{E}(\rho)$ from $\widetilde{\mathcal{E}}(\widetilde{\rho})$ rather than from $\mathcal{E}(\widetilde{\rho})$ [Fig. 2.1].

A further error bound can be obtained for the class of trace-preserving processes that do not increase the mean energy, acting on a set of input states whose mean energy does not exceed a certain value [51]. We illustrate this for a single optical mode (see Sec. 1.2.1). Suppose that the quantum states ρ of interest satisfy $\mathrm{Tr}[\rho \hat{H}] \leq U$. According to Ref. [51], if we choose the cutoff dimension $\dim(\widetilde{\mathscr{H}}) = N + 1$ such that $U/h_{N+1} \leq \gamma$ for some (small) $\gamma > 0$, the reconstructed process output errors are bounded from above as

$$\left\| \mathcal{E}(\rho) - \frac{\widetilde{\mathcal{E}}(\widetilde{\rho})}{\mathrm{Tr}\left[\widetilde{\mathcal{E}}(\widetilde{\rho})\right]} \right\|_1 \leq 2\epsilon, \tag{2.24}$$

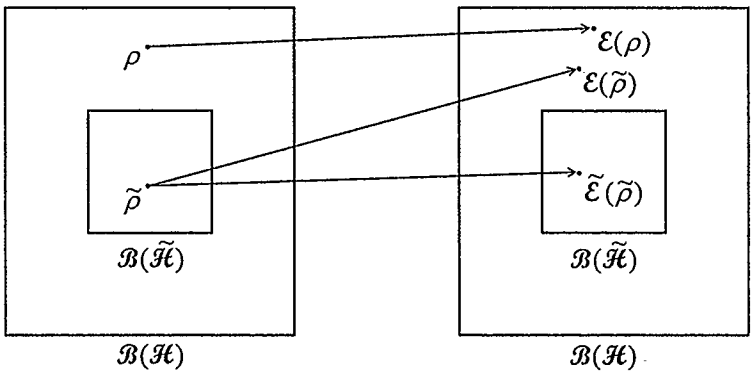

Figure 2.1: Errors associated with photon number cutoff. Restricting $\mathcal{B}(\mathcal{H})$ to $\mathcal{B}(\widetilde{\mathcal{H}})$ results in approximation $\widetilde{\rho}$ of the input state ρ. If the error of this approximation $\|\rho - \widetilde{\rho}\|_1$ is known, the error of the images $\|\mathcal{E}(\rho) - \mathcal{E}(\widetilde{\rho})\|_1$ can be estimated according to Eq. (2.23). However, the difference between $\mathcal{E}(\rho)$ and $\widetilde{\mathcal{E}}(\widetilde{\rho})$ in the cutoff space remains generally unknown.

where

$$\epsilon = 2\sqrt{\gamma} + \gamma/(1-\gamma). \tag{2.25}$$

Conversely, if we want to achieve a certain upper bound ϵ on the error of approximation, which corresponds to a lower bound on the desired accuracy of the process characterization, we first solve Eq. (2.25) for $\gamma = \gamma(\epsilon)$, and then find the minimum $N_\gamma \in \mathbb{N}$ such that $U/h_{N_\gamma+1} \leq \gamma$. Any cutoff dimension $N+1 > N_\gamma$ is then sufficient for our purpose. For $\gamma \ll 1$, $\epsilon \approx 2\sqrt{\gamma}$, which yields

$$\epsilon = O(1/\sqrt{N}). \tag{2.26}$$

This implies that the error of approximation scales as $1/\sqrt{N}$ with the cutoff dimension $N+1$.

For example, in order to achieve a 10% error in (2.24), we need $\epsilon = 0.05$ and thus $\gamma \approx 0.0006$. For the input mean energy bound corresponding to one photon ($U = 3/2\omega$), the required cutoff is $N \approx U/\gamma \approx 250$. This calculation shows that the above error estimate is extremely conservative.

2.4 Existence condition of the Glauber-Sudarshan representation

csQPT is based on using the Glauber-Sudarshan representation. Hence, we need to examine the condition for existence of the representation in more detail.

The diagonal coherent-state matrix elements of a density operator, $\langle\alpha'|\rho|\alpha'\rangle$, by using the Glauber-Sudarshan representation can be written as the following convolution integral form

$$\langle\alpha'|\rho|\alpha'\rangle = \int_{\mathbb{C}} \mathrm{d}^2\alpha \, P_\rho(\alpha) e^{-|\alpha'-\alpha|^2}. \tag{2.27}$$

The existence of the Glauber-Sudarshan representation for an arbitrary density matrix ρ reduces then to the inversion of Eq. (2.27).

In fact, the P-function for many density matrices only exists in terms of a *generalized function* or *distribution*, which can be defined on a set of functions called *test functions*. The function $e^{-|\alpha'-\alpha|^2}$ is in the Schwartz space of test functions of two variables. A Schwartz function is infinitely differentiable and the function and all its derivatives decay faster than any polynomial at infinity [52].

From Eq. (2.27), thus, the P-function must belong to the class of the generalized functions, which can be defined on the Schwartz space of test functions. This class of generalized functions is called *tempered distributions*. A distribution is tempered if and only if it can be identified with a derivative of finite order of a continuous function that is bounded by a polynomial [53]. The Fourier transform can be formally generalized to cover tempered distributions; the Fourier transform of a tempered distribution is again a tempered distribution. Therefore, a necessary and sufficient condition for Eq. (2.27) to possess a solution for any arbitrary operator is that the P-function be a tempered distribution.

For some quantum states the P-function is more singular than a tempered distribution, so it is not compatible with the form of the Glauber-Sudarshan representation [Eq. (2.27)]; hence, the representation does not exists. For example, the P-function for the superposition of two

coherent states

$$|\psi\rangle\langle\psi| = \frac{1}{N}(|\beta\rangle + |\gamma\rangle)(\langle\beta| + \langle\gamma|), \tag{2.28}$$

where N is the normalization factor and $\beta \neq \gamma$, is not a tempered distribution [54]. For the case of pure states it has been shown that the P-function is a tempered distribution when the state can be expressed as a linear combination of a finite number of the states $(\hat{a}^\dagger)^n|\alpha\rangle$ for arbitrary value of α [44].

The condition for existence of the P-function in the form of a tempered distribution is that the function $\langle\alpha|\rho|\alpha\rangle$ can be expressed as a sum of terms that each decreases less slowly than $e^{-|\alpha|^2}$ for large values of $|\alpha|$ [45]. When the function $\langle\alpha|\rho|\alpha\rangle$ contains a term that decreases more rapidly than $e^{-|\alpha|^2}$, some regularization is required [45, 46, 47].

If the P-function exists, it can be calculated using this formula [39]

$$P(\alpha) = \frac{e^{|\alpha|^2}}{\pi^2}\int \mathrm{d}^2\beta\langle-\beta|\rho|\beta\rangle e^{|\beta|^2-\beta\bar{\alpha}+\bar{\beta}\alpha}, \tag{2.29}$$

where $|\beta\rangle$ is coherent state and the integral is over the entire complex plane.

2.5 Conclusion

In this chapter, we have presented a mathematical representation for quantum processes in the form of a rank-4 tensor called the process tensor. In the case of symmetry, we discussed that the number of unknown elements in the process tensor reduces and also generalized this representation to the case of multi-mode processes.

In Sec. 2.3, we showed that, by employing a regularization operator, the process estimation can be restricted to a finite-dimensional subset of $\mathscr{B}(\mathscr{H})$. Hence, with sufficiently large amount of sampling, the estimate for the process output is a close approximation of the actual output state, which can be reconstructed by measurement devices. Furthermore, we considered the projection operator to the subspace of the Hilbert space with a fixed maximum number

N of photons as an example of the regularization operator. We showed that the accuracy of process estimation scales inversely with the square root of photon-number cutoff.

In Sec. 2.4, we examined the existence condition of the Glauber-Sudarshan representation. We showed the necessary and sufficient condition for existence of the representation is that $\langle\alpha|\rho|\alpha\rangle$ decreases less slowly than $e^{-|\alpha|^2}$ for large value of $|\alpha|$.

Chapter 3

New method for csQPT

This chapter introduces our new method for csQPT [14]. In this method, based on finding effect of an unknown quantum-optical process on coherent states $\varrho_{\mathcal{E}}(\alpha)$ [Eq. (1.14)], we provide a new procedure for determining the process tensor in the Fock basis.

We study general quantum optical processes $\mathcal{E}$ acting on quantum states of light and begin with the simplest case for which only a single electromagnetic-field mode is involved. Next, in Sec. 3.1.1, we consider the multi-mode generalization. In Sec. 3.1.2, we show that, in principle, knowing the effect of the process on coherent states with low amplitude around the origin in the phase space is enough to calculate the process tensor. In Sec. 3.2, we illustrate our technique by finding the corresponding superoperator for some important quantum-optical processes. In the last section, we conclude this chapter and compare our method with the original proposal [13].

The results of my project presented in this chapter are as follows:

- a new method for calculating the superoperator of an unknown quantum-optical process in the Fock basis based on using coherent states as probe states (csQPT),
- multi-mode generalization of the method,
- showing the representation $\langle j|\varrho_{\mathcal{E}}(\alpha)|k\rangle$ is an entire function,
- calculation of the superoperators for some fundamental quantum-optical processes (identity, attenuation, photon subtraction, photon addition, Schrödinger-cat generation, beam splitter, parametric down conversion).

3.1 Formalism: determining the quantum process tensor

In this section, we introduce a new formulation for csQPT. This formulation is based on using the Fock basis $\{|n\rangle\}$ to represent completely positive map

$$\mathcal{E}_{jk}^{mn} = \langle j|\mathcal{E}(|m\rangle\langle n|)|k\rangle, \tag{3.1}$$

where $n, m, j, k \in \mathbb{N}_0$.

In what follows, we show how to estimate the process tensor elements $\mathcal{E}(|m\rangle\langle n|)$ for m, n within a finite domain $\{0, \ldots, N\}$. Regarding to the existence condition for the Glauber-Sudarshan representation (Sec. 2.4), because

$$\langle\alpha|(|m\rangle\langle n|)|\alpha\rangle = e^{-|\alpha|^2}\frac{\alpha^n\bar{\alpha}^m}{\sqrt{m!n!}} \tag{3.2}$$

decreases less slowly than $e^{-|\alpha|^2}$ (for large $|\alpha|$), the Glauber-Sudarshan P representation

$$|m\rangle\langle n| = \int_{\mathbb{C}} \mathrm{d}^2\alpha\, P_{mn}(\alpha)|\alpha\rangle\langle\alpha| \tag{3.3}$$

is guaranteed to exist for any operator $|m\rangle\langle n|$ (see Sec. 2.4).

The P-function can be calculated by means of Eq. (2.29):

$$\begin{aligned}
P_{mn}(\alpha) &= \frac{e^{|\alpha|^2}}{\pi^2}\int_{\mathbb{C}} \mathrm{d}^2\beta\, \langle -\beta|m\rangle\langle n|\beta\rangle e^{|\beta|^2-\beta\bar{\alpha}+\bar{\beta}\alpha} \\
&= \frac{(-1)^m e^{|\alpha|^2}}{\pi^2\sqrt{m!n!}}\int_{\mathbb{C}} \mathrm{d}^2\beta\, \bar{\beta}^m\beta^n e^{-\beta\bar{\alpha}+\bar{\beta}\alpha} \\
&= \frac{(-1)^{m+n} e^{|\alpha|^2}}{\pi^2\sqrt{m!n!}}\partial_\alpha^m\partial_{\bar{\alpha}}^n\int_{\mathbb{C}} \mathrm{d}^2\beta\, e^{-\beta\bar{\alpha}+\bar{\beta}\alpha} \\
&= (-1)^{m+n}\frac{e^{|\alpha|^2}}{\sqrt{m!n!}}\partial_\alpha^m\partial_{\bar{\alpha}}^n\delta^2(\alpha)
\end{aligned} \tag{3.4}$$

for $\partial_\alpha^m := \partial^m/\partial\alpha^m$ and α and its complex conjugate $\bar{\alpha}$ treated as independent variables, and $\delta^2(\alpha) \equiv \delta(\mathrm{Re}(\alpha))\delta(\mathrm{Im}(\alpha))$.

From representation (3.3) and exploiting linearity of the process, we obtain

$$\mathcal{E}\left(|m\rangle\langle n|\right) = \int_{\mathbb{C}} \mathrm{d}^2\alpha\, P_{mn}(\alpha)\varrho_{\mathcal{E}}(\alpha), \tag{3.5}$$

where $\varrho_{\mathcal{E}}(\alpha)$ is defined in Eq. (1.14). By inserting this equation into Eq. (3.1), we obtain the process tensor

$$\mathcal{E}_{jk}^{mn} = \int_{\mathbb{C}} \mathrm{d}^2\alpha \, P_{mn}(\alpha) \langle j|\varrho_{\mathcal{E}}(\alpha)|k\rangle. \tag{3.6}$$

This expression can be simplified by using Eq. (3.4) and performing integration by parts:

$$\begin{aligned} \mathcal{E}_{jk}^{mn} &= \int_{\mathbb{C}} \mathrm{d}^2\alpha \, \frac{\delta^2(\alpha)}{\sqrt{m!n!}} \partial_{\alpha}^{m} \partial_{\bar{\alpha}}^{n} \left[e^{|\alpha|^2} \langle j|\varrho_{\mathcal{E}}(\alpha)|k\rangle \right] \\ &= \frac{1}{\sqrt{m!n!}} \partial_{\alpha}^{m} \partial_{\bar{\alpha}}^{n} \left[e^{|\alpha|^2} \langle j|\varrho_{\mathcal{E}}(\alpha)|k\rangle \right] \Big|_{\alpha=0}. \end{aligned} \tag{3.7}$$

In this thesis, $\langle j|\varrho_{\mathcal{E}}(\alpha)|k\rangle$ is referred to as "hybrid coherent-Fock state representation".

Thus we have eliminated the need to make use of the Glauber-Sudarshan representation for quantum states and the need to regularize the P-function. Hence, this method improves the accuracy compared to Ref. [13] by removing the error associated with the regularization. The process tensor is found by taking partial derivatives (with respect to α and $\bar{\alpha}$) of the matrix elements of $\varrho_{\mathcal{E}}(\alpha)$, which are estimated from experimental data and evaluated at $\alpha = 0$.

Furthermore, the mathematical procedure defined by Eq. (3.7) is simpler and computationally faster (see Sec. 4.2) than employing Eq. (3.6) with a regularized version of $P_{L,mn}(\alpha)$ replacing the tempered distribution $P_{mn}(\alpha)$ [13, 42]. Equation (3.7) has been used to determine the fidelity of quantum teleportation of a single-rail optical qubit based on measurements performed on coherent states (see supplementary material in Ref. [55]).

The above formalism is not restricted to trace-preserving quantum processes. Indeed, trace preservation was not required in the derivation of our results. Thus, our method is applicable to all quantum optical processes that are mathematically described by completely-positive maps, but may be trace-preserving, trace-reducing or even trace-increasing. Non-trace-preserving quantum processes are either *conditional processes* or part of a larger process $\mathcal{E} = \sum_i \mathcal{E}_i$, which is trace-preserving as a whole but whose components $\mathcal{E}_i$ may increase or decrease the trace, respectively. A conditional process is a process that is conditioned on a certain probabilistic event; for example, it may be heralded if the event is observed. One notable examples

of such a process is a probabilistic conditional-NOT gate (CNOT), which forms the basis for the Knill-Laflamme-Milburn linear-optical quantum computing scheme [49]. Other examples are photon-addition and photon-subtraction processes, whose superoperators are derived in Sec. 3.2.

In experimental csQPT, states $\varrho_{\mathcal{E}}(\alpha)$ are determined using homodyne tomography [22]. It is important to remember, however, that this procedure reconstructs a density matrix normalized to unit trace:

$$\widetilde{\varrho}_{\mathcal{E}}(\alpha) = \frac{\varrho_{\mathcal{E}}(\alpha)}{\mathrm{Tr}\left[\varrho_{\mathcal{E}}(\alpha)\right]}. \tag{3.8}$$

When measuring non-trace-preserving processes, one must recover the trace information contained in $\varrho_{\mathcal{E}}(\alpha)$. This information can be obtained by measuring the probability $p_{\alpha}(\mathcal{E}) = \mathrm{Tr}\left[\varrho_{\mathcal{E}}(\alpha)\right]$ of the process heralding event for all α's for which the measurements are performed. The state to be used in Eq. (3.7) in place of $\varrho_{\mathcal{E}}(\alpha)$ is then $\widetilde{\varrho}_{\mathcal{E}}(\alpha)\mathrm{Tr}\left[\varrho_{\mathcal{E}}(\alpha)\right]$.

3.1.1 Multi-mode generalization

The use of quantum process tomography is not restricted to the single-mode cases. In some applications, we need to find the effect of the process on the multi-mode quantum states. For example, in a dual-rail qubit, the information is encoded in two different modes of oscillation; hence, to verify performance of the quantum gate acting on a dual-rail qubit, two-mode process tomography is required.

Generalization of our method to the multi-mode case is straightforward. In the M-mode case, we use the notation $|n\rangle$ (with $n \in \mathbb{N}_0^M$) for multi-mode Fock states and $|\alpha\rangle := |\alpha_1, \alpha_2, \ldots, \alpha_M\rangle$ (with $\alpha \in \mathbb{C}^M$) for multi-mode coherent states. The M-mode process tensor in the Fock basis is

$$\mathcal{E}_{jk}^{mn} = \langle j|\mathcal{E}(|m\rangle\langle n|)|k\rangle. \tag{3.9}$$

Similar to the single-mode case, we employ the Glauber-Sudarshan P representation for

the multi-mode operator $|m\rangle\langle n|$,

$$|m\rangle\langle n| = \prod_{s=1}^{M} \int_{\mathbb{C}} \mathrm{d}^2\alpha_s \, P_{mn}(\alpha)|\alpha\rangle\langle\alpha|, \tag{3.10}$$

with the overall P-function being a product of the P-functions for the constituent modes:

$$P_{mn}(\alpha) = \prod_{s=1}^{M} \frac{e^{|\alpha_s|^2}(-1)^{m_s+n_s}}{\sqrt{m_s!n_s!}} \partial_{\alpha_s}^{m_s} \partial_{\bar{\alpha}_s}^{n_s} \delta^2(\alpha_s). \tag{3.11}$$

From Eq. (3.9) and performing multiple integration by parts, we obtain

$$\begin{aligned} \mathcal{E}_{jk}^{mn} &= \int_{\mathbb{C}^M} \mathrm{d}^{2M}\alpha \prod_{s=1}^{M} \frac{\delta^2(\alpha_s)}{\sqrt{m_s!n_s!}} \partial_{\alpha_s}^{m_s} \partial_{\bar{\alpha}_s}^{n_s} \left[e^{|\alpha_s|^2} \langle j|\varrho_{\mathcal{E}}(\alpha)|k\rangle \right] \\ &= \prod_{s=1}^{M} \frac{1}{\sqrt{m_s!n_s!}} \partial_{\alpha_s}^{m_s} \partial_{\bar{\alpha}_s}^{n_s} \left[e^{|\alpha_s|^2} \langle j|\varrho_{\mathcal{E}}(\alpha)|k\rangle \right] \Big|_{\alpha_s=0}, \end{aligned} \tag{3.12}$$

where

$$\varrho_{\mathcal{E}}(\alpha) \equiv \mathcal{E}(|\alpha\rangle\langle\alpha|). \tag{3.13}$$

Equations (3.7) and (3.12) complete our coherent-state tomography formalism and show that coherent states provide a complete set of probe states for characterizing quantum optical processes, insofar as the expression for $\varrho_{\mathcal{E}}(\alpha)$ completely determines the process tensor.

3.1.2 Hybrid coherent-Fock state representation as an entire function

According to Eq. (3.7), by knowing the hybrid coherent-Fock state representation ($\langle j|\varrho_{\mathcal{E}}(\alpha)|k\rangle$) as a complex-valued function of the variable α for any j and k, one can determine the process tensor $\mathcal{E}_{jk}^{mn}$. An interesting feature of Eqs. (3.7) and (3.12) is that complete information about a quantum optical process is contained in its action on an infinitesimally-small compact set of all probe coherent states in the immediate vicinity of the vacuum state $|0\rangle$ [Fig. 3.1]. From a mathematical point of view, this feature can be understood by realizing that, for any $j, k \in \mathbb{N}_0$, the hybrid coherent-Fock state representation is an *entire function*, i.e., a complex-valued function in the variables $\alpha, \bar{\alpha}$ that is holomorphic over the whole complex plane, and so is its product

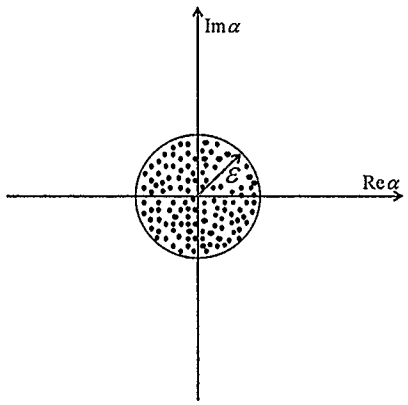

Figure 3.1: Each point represents a coherent state in the phase space. The effects of a quantum process on the coherent states within distance ε from the vacuum state are only required to characterize the process.

with the exponential $e^{|\alpha|^2}$. Here we show this function is entire so it can be represented as a power series that converges uniformly on any compact domain.

As a completely-positive quantum operation, $\mathcal{E}$ possesses a Kraus decomposition Eq. (2.3); hence we can rewrite the hybrid coherent-Fock state representation as

$$\begin{aligned}\langle j|\varrho_{\mathcal{E}}(\alpha)|k\rangle &= \sum_{i=1}^{L}\langle j|\hat{K}_i|\alpha\rangle\langle\alpha|\hat{K}_i^\dagger|k\rangle \\ &= \sum_{i=1}^{L}\langle\alpha|\hat{K}_i^\dagger|k\rangle\langle j|\hat{K}_i|\alpha\rangle \\ &= \langle\alpha|\mathcal{E}_*(|k\rangle\langle j|)|\alpha\rangle, \end{aligned} \tag{3.14}$$

where

$$\mathcal{E}_* : \mathscr{B}(\mathscr{H}) \to \mathscr{B}(\mathscr{H}) \; : \; \hat{B} \mapsto \sum_{i=1}^{L}\hat{K}_i^\dagger\,\hat{B}\,\hat{K}_i, \tag{3.15}$$

is the dual or adjoint map [56]. The complex-valued function $\langle\alpha|\hat{A}|\alpha\rangle$ (referred to as a Q-symbol if $\hat{A}$ is a density operator)—where $\hat{A}$ is any bounded operator on $\mathcal{H}$—is an entire function of the two variables α and $\bar{\alpha}$ [43, 39]. Hence the right-hand side of Eq. (3.14) implies that the function $\langle j|\varrho_{\mathcal{E}}(\alpha)|k\rangle$ is an entire function. By representing the coherent states in

Eq. (3.14) in the Fock basis and using Eq. (3.1), we obtain

$$\langle j|\varrho_{\mathcal{E}}(\alpha)|k\rangle = e^{-|\alpha|^2}\sum_{n=0}^{\infty}\sum_{m=0}^{\infty}\frac{\alpha^n\bar{\alpha}^m}{\sqrt{n!m!}}\mathcal{E}_{jk}^{nm}, \tag{3.16}$$

which is a power series of the complex variables α and $\bar{\alpha}$, hence convergent everywhere [43, 39].

Thus, each term $e^{|\alpha|^2}\langle j|\varrho_{\mathcal{E}}(\alpha)|k\rangle$ is infinitely differentiable over the whole complex plane and is identical to its Taylor series expansion for any element of $\mathbb{C}$. Moreover, Eq. (3.7) implies that the process tensor is determined by the corresponding Taylor coefficients at $\alpha = 0$. The same conclusion applies to the multi-mode case, for which we deal with entire functions on $\mathbb{C}^M$.

3.2 Examples: superoperators of important quantum optical processes

In this section, we illustrate our new method by applying it to some fundamental quantum optical processes whose effects on coherent states are known. Specifically, using Eqs. (3.7) or (3.12), we analytically derive corresponding superoperator tensors $\mathcal{E}_{jk}^{mn}$ in the Fock basis. The results are summarized in Table 3.1.

3.2.1 Identity

For the identity process ($\mathcal{E}_{\mathcal{I}}$), the effect of process on coherent states is $\varrho_{\mathcal{E}_{\mathcal{I}}}(\alpha) = |\alpha\rangle\langle\alpha|$. Then the matrix elements of the output states are

$$\langle j|\varrho_{\mathcal{E}_{\mathcal{I}}}(\alpha)|k\rangle = e^{-|\alpha|^2}\frac{\alpha^j\bar{\alpha}^k}{\sqrt{j!k!}}. \tag{3.17}$$

Inserting these elements into Eq. (3.7) yields $\mathcal{E}_{jk}^{mn} = \delta_{mj}\delta_{nk}$ as expected.

3.2.2 Attenuation and lossy channel

For attenuation of light fields ($\mathcal{E}_{\rm att}$), the process's effect on single-mode coherent states is given by $\varrho_{\mathcal{E}_{\rm att}}(\alpha) = |\eta\alpha\rangle\langle\eta\alpha|$, where $0 \leq \eta < 1$. The matrix elements in the Fock basis are

$$\langle j|\varrho_{\mathcal{E}_{\rm att}}(\alpha)|k\rangle = e^{-\eta^2|\alpha|^2}\frac{\eta^{j+k}\alpha^j\bar{\alpha}^k}{\sqrt{j!k!}} \,. \tag{3.18}$$

From Eq. (3.7), we obtain

$$\begin{aligned}\mathcal{E}_{jk}^{mn} &= \frac{\eta^{j+k}}{\sqrt{m!n!j!k!}}\partial_\alpha^m\partial_{\bar{\alpha}}^n\left[e^{|\alpha|^2(1-\eta^2)}\alpha^j\bar{\alpha}^k\right]\Big|_{\alpha,\bar{\alpha}=0} \\ &= \frac{\eta^{j+k}}{\sqrt{m!n!j!k!}}\partial_\alpha^m\partial_{\bar{\alpha}}^n\sum_{l=0}^{\infty}\frac{(1-\eta^2)^l\alpha^{j+l}\bar{\alpha}^{k+l}}{l!}\Big|_{\alpha,\bar{\alpha}=0} \\ &= \sqrt{\frac{m!n!}{j!k!}}\frac{\eta^{j+k}(1-\eta^2)^{m-j}}{(m-j)!}\delta_{m-j,n-k}\,,\end{aligned} \tag{3.19}$$

which depends explicitly on η.

3.2.3 Photon subtraction and addition

Photon subtraction is defined as a process that removes a single photon from the light field, whereas photon addition adds a single photon. Photon subtraction has been used by Ourjoumtsev et al. [57] to generate optical Schrödinger kittens (coherent superpositions of low-amplitude coherent states) from squeezed vacuum states for the purpose of quantum information processing. Single-photon-added coherent states can be regarded as the result of the most elementary amplification process of classical light fields by a single quantum of excitation; being intermediate between single-photon Fock states (fully quantum-mechanical) and coherent (classical) ones, these states have been demonstrated to be suited for the study of the smooth transition between particle-like and wavelike behavior of light [58].

Here we discuss idealized single-mode photon subtraction and photon addition. Both processes are non-trace-preserving. For example, photon subtraction can be approximately realized [57] by a highly-transmissive beam splitter whose reflected mode is directed to a detector

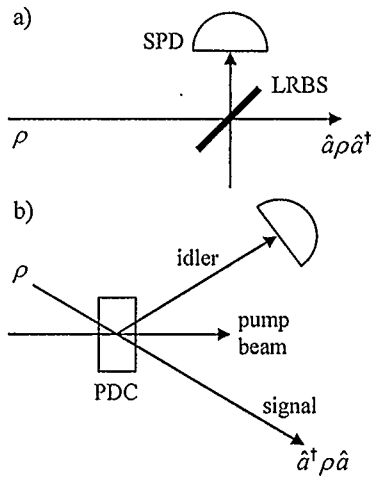

Figure 3.2: (a) Experimental realization of photon subtraction; using low reflectivity beam splitter (LRBS) the photon subtraction process is heralded by a single-photon detector (SPD) click. (b) Experimental realization of photon addition; the photon addition process is heralded by a SPD click of the idler mode of the parametric down-conversion (PDC).

and whose transmitted mode constitutes the output, respectively, as illustrated in Fig. 3.2a. Any click of a detector implies extraction of photon(s) from the input mode by the beam splitter. As the beam splitter has low reflectivity, here single-photon extraction events are more likely than multi-photon events. An approximate experimental realization of photon addition is illustrated in Fig. 3.2b. The input quantum state ρ enters the signal channel of a parametric down-conversion setup with the low parametric gain [58]. Provided that detector dark counts are neglected, a photon detection of the idler mode heralds photon addition to the signal mode, which contains the output state of the process.

The effect of photon subtraction ($\mathcal{E}_{\text{sub}}$) and addition ($\mathcal{E}_{\text{add}}$) on coherent states is given by $\varrho_{\mathcal{E}_{\text{sub}}}(\alpha) = \hat{a}|\alpha\rangle\langle\alpha|\hat{a}^\dagger$ and $\varrho_{\mathcal{E}_{\text{add}}}(\alpha) = \hat{a}^\dagger|\alpha\rangle\langle\alpha|\hat{a}$, respectively, where $\hat{a}$ and $\hat{a}^\dagger$ are the photon annihilation and photon creation operators of a single mode, respectively. The matrix elements

of the output states in the Fock basis are

$$\langle j|\varrho_{\mathcal{E}_{\rm sub}}(\alpha)|k\rangle = e^{-|\alpha|^2}\frac{\alpha^{j+1}\bar{\alpha}^{k+1}}{\sqrt{j!k!}}, \tag{3.20}$$

$$\langle j|\varrho_{\mathcal{E}_{\rm add}}(\alpha)|k\rangle = e^{-|\alpha|^2}\sqrt{kj}\frac{\alpha^{j-1}\bar{\alpha}^{k-1}}{\sqrt{(j-1)!(k-1)!}}. \tag{3.21}$$

The process tensor is

$$\mathcal{E}_{jk}^{mn} = \begin{cases} \sqrt{(j+1)(k+1)}\delta_{m,j+1}\delta_{n,k+1}, & \text{for photon subtraction,} \\ \sqrt{kj}\delta_{m,j-1}\delta_{n,k-1}, & \text{for photon addition,} \end{cases} \tag{3.22}$$

where we have employed Eq. (3.7).

3.2.4 Schrödinger-cat generation

The unitary evolution according to $\hat{U}_{\rm Kerr}(\chi) \equiv \exp\left[-i\chi\left(\hat{a}^\dagger\hat{a}\right)^2\right]$ for $\chi = \pi/2$, if applied to coherent states, generates Schrödinger-cat states (hereafter denoted as $\mathcal{E}_{\rm cat}$) [59, 60]

$$\begin{aligned}\varrho_{\mathcal{E}_{\rm cat}}(\alpha) &= \hat{U}_{\rm Kerr}\left(\frac{\pi}{2}\right)|\alpha\rangle\langle\alpha|\hat{U}_{\rm Kerr}^\dagger\left(\frac{\pi}{2}\right) \\ &= \frac{1}{2}\left(|\alpha\rangle + i|-\alpha\rangle\right)\left(\langle\alpha| - i\langle-\alpha|\right),\end{aligned} \tag{3.23}$$

with matrix elements

$$\langle j|\varrho_{\mathcal{E}_{\rm cat}}(\alpha)|k\rangle = \frac{e^{-|\alpha|^2}\alpha^j\bar{\alpha}^k}{2\sqrt{j!k!}}\left[1 + (-1)^{j+k} + i(-1)^j - i(-1)^k\right]. \tag{3.24}$$

The superoperator tensor for this non-Gaussian unitary process obtained via Eq. (3.7) is

$$\mathcal{E}_{jk}^{mn} = e^{-i\frac{\pi}{2}(j^2-k^2)}\delta_{mj}\delta_{nk}. \tag{3.25}$$

This process does not change the total particle number of any input state.

3.2.5 Beam splitter

Now let us consider the beam splitter as an example of a two-mode process. The unitary beam splitter transformation is given by [61]

$$\hat{B}(\Theta) = e^{\frac{\Theta}{2}(\hat{a}_2^\dagger\hat{a}_1 - \hat{a}_1^\dagger\hat{a}_2)}, \tag{3.26}$$

where Θ is the beam splitter reflection parameter. Specifically, its action on coherent state inputs $|\alpha_1\rangle$ and $|\alpha_2\rangle$ is given as

$$\begin{aligned}\varrho_{\mathcal{E}_B S}(\alpha_1,\alpha_2) =& \mathcal{E}_B\left(|\alpha_1,\alpha_2\rangle\langle\alpha_1,\alpha_2|\right)\\ =& \hat{B}^\dagger(\Theta)\left(|\alpha_1,\alpha_2\rangle\langle\alpha_1,\alpha_2|\right)\hat{B}(\Theta)\\ =& |T\alpha_1 - R\alpha_2, R\alpha_1 + T\alpha_2\rangle\langle T\alpha_1 - R\alpha_2, R\alpha_1 + T\alpha_2| \end{aligned} \tag{3.27}$$

with $T \equiv \cos(\Theta/2)$ and $R \equiv -\sin(\Theta/2)$ being the transmissivity and reflectivity, respectively. The matrix elements of the output states are

$$\begin{aligned}&\langle j_1, j_2|T\alpha_1 - R\alpha_2, R\alpha_1 + T\alpha_2\rangle\\ &\times\langle T\alpha_1 - R\alpha_2, R\alpha_1 + T\alpha_2|k_1,k_2\rangle = \frac{e^{-|\alpha_1|^2-|\alpha_2|^2}}{\sqrt{j_1!j_2!k_1!k_2!}}\left(T\alpha_1 - R\alpha_2\right)^{j_1}\left(R\alpha_1 + T\alpha_2\right)^{j_2}\\ &\qquad\times\left(T\bar{\alpha}_1 - R\bar{\alpha}_2\right)^{k_1}\left(R\bar{\alpha}_1 + T\bar{\alpha}_2\right)^{k_2}. \end{aligned} \tag{3.28}$$

From the effect of the process on two-mode coherent states, we calculate the corresponding tensor using Eq. (3.12), which yields

$$\begin{aligned}\mathcal{E}^{m_1m_2n_1n_2}_{j_1j_2k_1k_2} =& \sqrt{\frac{m_1!m_2!n_1!n_2!}{j_1!j_2!k_1!k_2!}}\sum_{p=0}^{j_1}\sum_{q=0}^{k_1}\binom{j_1}{p}\binom{j_2}{m_1-p}\binom{k_1}{q}\\ &\times\binom{k_2}{n_1-q}T^{2p+2q+j_2+k_2-m_1-n_1}\\ &\times(-1)^{j_1+k_1-p-q}R^{j_1+k_1+m_1+n_1-2p-2q}\\ &\times\delta_{m_1+m_2,j_1+j_2}\delta_{n_1+n_2,k_1+k_2}, \end{aligned} \tag{3.29}$$

as an explicit function of T and R.

3.2.6 Parametric down-conversion

Another two-mode process of interest is parametric down-conversion (PDC). In PDC, a crystal with an appreciably large second-order non-linearity is pumped by a laser field. Each of the pump photons can spontaneously decay into a pair of identical (degenerate PDC) or

nonidentical photons (nondegenerate PDC). Here we consider a nondegenerate PDC process $\mathcal{E}_{\text{PDC}}$ induced by the transformation [61]

$$\hat{S}_2(r) = e^{r(\hat{a}_1\hat{a}_2 - \hat{a}_1^\dagger\hat{a}_2^\dagger)}. \tag{3.30}$$

The effect of this unitary process on a two-mode coherent state is given by

$$\begin{aligned}\varrho_{\mathcal{E}_{\text{PDC}}}(\alpha_1,\alpha_2) &= \mathcal{E}_{\text{PDC}}(|\alpha_1,\alpha_2\rangle\langle\alpha_1,\alpha_2|) \\ &= \hat{S}_2(r)|\alpha_1,\alpha_2\rangle\langle\alpha_1,\alpha_2|\hat{S}_2^\dagger(r).\end{aligned} \tag{3.31}$$

To obtain the Fock representation of the PDC process, we first find the matrix elements of the output states in the Fock basis:

$$\begin{aligned}\langle j_1,j_2|\varrho_{\mathcal{E}_{\text{PDC}}}(\alpha_1,\alpha_2)|k_1,k_2\rangle &= \langle j_1,j_2|\hat{S}_2(r)|\alpha_1,\alpha_2\rangle\langle\alpha_1,\alpha_2|\hat{S}_2^\dagger(r)|k_1,k_2\rangle \\ &= I \times \bar{J},\end{aligned} \tag{3.32}$$

where $I := \langle\alpha_1,\alpha_2|\hat{S}_2^\dagger(r)|k_1,k_2\rangle$ and $J := \langle\alpha_1,\alpha_2|\hat{S}_2^\dagger(r)|j_1,j_2\rangle$. Employing the relations [63]

$$\hat{S}_2^\dagger(r)|0,0\rangle = \frac{1}{\cosh r}\sum_{l=0}^{\infty}(\tanh r)^l|l,l\rangle, \tag{3.33}$$

$$\hat{S}_2^\dagger(r)\hat{a}_1\hat{S}_2(r) = \hat{a}_1\cosh r - \hat{a}_2^\dagger\sinh r, \tag{3.34}$$

$$\hat{S}_2^\dagger(r)\hat{a}_2\hat{S}_2(r) = \hat{a}_2\cosh r - \hat{a}_1^\dagger\sinh r, \tag{3.35}$$

and the binomial expansion, we obtain

$$\begin{aligned}I =& \langle\alpha_1,\alpha_2|\hat{S}_2^\dagger(r)\frac{(\hat{a}_1^\dagger)^{k_1}}{\sqrt{k_1!}}\frac{(\hat{a}_2^\dagger)^{k_2}}{\sqrt{k_2!}}\hat{S}_2(r)\hat{S}_2^\dagger(r)|0,0\rangle \\ =& \frac{1}{\cosh r\sqrt{k_1!k_2!}}\sum_{l=0}^{\infty}(\tanh r)^l\langle\alpha_1\alpha_2|\sum_{p=0}^{k_1}\binom{k_1}{p}(\hat{a}_1^\dagger\cosh r)^{k_1-p}(-\hat{a}_2\sinh r)^p \\ &\times\sum_{q=0}^{k_2}\binom{k_2}{q}(\hat{a}_2^\dagger\cosh r)^{k_2-q}(-\hat{a}_1\sinh r)^q|l,l\rangle.\end{aligned} \tag{3.36}$$

Using

$$\hat{a}^x|l\rangle = \sqrt{\frac{l!}{(l-x)!}}|l-x\rangle \tag{3.37}$$

and

$$(\hat{a}^\dagger)^y|l\rangle = \sqrt{\frac{(l+y)!}{l!}}|l+y\rangle \tag{3.38}$$

we obtain:

$$\begin{aligned} I =& \frac{1}{\cosh r\sqrt{k_1!k_2!}} \sum_{l=0}^{\infty} (\tanh r)^l \sum_{p=0}^{k_1} \binom{k_1}{p} (\cosh r)^{k_1-p} (-\sinh r)^p \\ & \times \sum_{q=0}^{k_2} \binom{k_2}{q} (\cosh r)^{k_2-q} (-\sinh r)^q e^{-|\alpha_1|^2/2-|\alpha_2|^2/2} \\ & \times \bar{\alpha}_1^{l+k_1-q-p} \bar{\alpha}_2^{l+k_2-q-p} \frac{(l+k_2-q)!}{(l-q)!(l+k_2-q-p)!} \,. \end{aligned} \tag{3.39}$$

From the symmetry between I and J, and by replacing k_1 and k_2 by j_1 and j_2, respectively, we also find:

$$\begin{aligned} \bar{J} =& \frac{1}{\cosh r\sqrt{j_1!j_2!}} \sum_{l'=0}^{\infty} (\tanh r)^{l'} \sum_{u=0}^{j_1} \binom{j_1}{u} (\cosh r)^{j_1-u} (-\sinh r)^u \\ & \times \sum_{v=0}^{j_2} \binom{j_2}{v} (\cosh r)^{j_2-v} (-\sinh r)^v \, e^{-|\alpha_1|^2/2-|\alpha_2|^2/2} \\ & \times \alpha_1^{l'+j_1-u-v} \alpha_2^{l'+j_2-u-v} \frac{(l'+j_2-v)!}{(l'-v)!\,(l'+j_2-u-v)!} \,. \end{aligned} \tag{3.40}$$

The Fock representation of the superoperator for the PDC process is then given by

$$\begin{aligned}
\mathcal{E}^{m_1 m_2 n_1 n_2}_{j_1 j_2 k_1 k_2} =& \frac{1}{\sqrt{m_1! m_2! n_1! n_2!}} \partial^{m_1}_{\alpha_1} \partial^{n_1}_{\bar{\alpha}_1} \partial^{m_2}_{\alpha_2} \partial^{n_2}_{\bar{\alpha}_2} \left(e^{|\alpha_1|^2 + |\alpha_2|^2} I \times \bar{J} \right) \Big|_{\alpha_1, \alpha_2 = 0} \\
=& \sqrt{\frac{n_1! m_1!}{n_2! m_2!}} \frac{1}{\cosh r^2 \sqrt{j_1! j_2! k_1! k_2!}} \sum_{p=0}^{k_1} \binom{k_1}{p} (\cosh r)^{k_1 - p} (-\sinh r)^p \\
& \times (\tanh r)^{n_1 - k_1 + p} \frac{(n_1 - k_1 + k_2 + p)!}{(n_1 - k_1 + p)!} \delta_{n_1 - n_2, k_2 - k_2} \\
& \times \sum_{q=0}^{k_2} \binom{k_2}{q} (\cosh r)^{k_2 - q} (-\sinh r \tanh r)^q \\
& \times \sum_{u=0}^{j_1} \binom{j_1}{u} (\cosh r)^{j_1 - u} (-\sinh r)^u (\tanh r)^{m_1 - j_1 + u} \frac{(m_1 - j_1 + j_2 + u)!}{(m_1 - j_1 + u)!} \\
& \times \delta_{m_2 - m_1, j_2 - j_1} \sum_{v=0}^{j_2} \binom{j_2}{v} (\cosh r)^{j_2 - v} (-\sinh r \tanh r)^v \\
=& \sqrt{\frac{n_1! m_1! k_1! j_1!}{n_2! m_2! k_2! j_2!}} \frac{(\tanh r)^{n_1 + m_1}}{(\cosh r)^{k_2 + j_2 + 2}} \\
& \times \sum_{p=0}^{k_1} \sum_{u=0}^{j_1} \frac{(\frac{\cosh r}{\tanh r})^{k_1 + j_1 - p - u} (-\sinh r)^{p+u}}{p!\,(k_1 - p)!\,u!\,(j_1 - u)!} \\
& \times \frac{(n_2 + p)!\,(m_2 + u)!}{(n_1 - k_1 + p)!\,(m_1 - j_1 + u)!} \delta_{n_2 - n_1, k_2 - k_1}\, \delta_{m_2 - m_1, j_2 - j_1}\,,
\end{aligned} \tag{3.41}$$

which can also be expressed in terms of a product of values of the hypergeometric function ${}_2F_1$, as given by

$$\begin{aligned}
\mathcal{E}^{m_1 m_2 n_1 n_2}_{j_1 j_2 k_1 k_2} =& \sqrt{\frac{n_1! m_1! m_2! n_2!}{j_1! k_1! k_2! j_2!}} \frac{(\tanh r)^{m_1 + n_1 - j_1 - k_1}}{(m_1 - j_1)!\,(n_1 - k_1)!\,(\cosh r)^{j_2 + k_2 - j_1 - k_1 + 2}} \\
& \times {}_2F_1\left(-j_1, m_2 + 1; m_1 - j_1 + 1; \tanh^2 r\right) \\
& \times {}_2F_1\left(-k_1, n_2 + 1; n_1 - k_1 + 1; \tanh^2 r\right) \\
& \times \delta_{m_2 - m_1, j_2 - j_1}\, \delta_{n_2 - n_1, k_2 - k_1}\,,
\end{aligned} \tag{3.42}$$

with

$${}_2F_1(\alpha, \beta; \gamma; z) := 1 + \sum_{n=1}^{\infty} \frac{(\alpha)_n (\beta)_n}{(\gamma)_n} \frac{z^n}{n!}\,, \tag{3.43}$$

Table 3.1: Process tensor $\mathcal{E}_{jk}^{mn}$ for some quantum optical processes

Operation $\mathcal{E}$	$\varrho_{\mathcal{E}}(\alpha)$	Process tensor $\mathcal{E}_{jk}^{mn}$
Identity ($\mathcal{E}_{\mathcal{I}}$)	$\|\alpha\rangle\langle\alpha\|$	$\delta_{mj}\delta_{nk}$
Attenuation ($\mathcal{E}_{\text{att}}$)	$\|\eta\alpha\rangle\langle\eta\alpha\|$	$\sqrt{\frac{m!n!}{j!k!}}\frac{\eta^{j+k}(1-\eta^2)^{m-j}}{(m-j)!}\delta_{m-j,n-k}$
Photon addition ($\mathcal{E}_{\text{add}}$)	$\hat{a}^\dagger\|\alpha\rangle\langle\alpha\|\hat{a}$	$\sqrt{kj}\delta_{m,j-1}\delta_{n,k-1}$
Photon subtraction ($\mathcal{E}_{\text{sub}}$)	$\hat{a}\|\alpha\rangle\langle\alpha\|\hat{a}^\dagger$	$\sqrt{(j+1)(k+1)}\delta_{m,j+1}\delta_{n,k+1}$
Cat generation ($\mathcal{E}_{\text{cat}}$)	$\frac{1}{2}(\|\alpha\rangle + i\|-\alpha\rangle)$ $\times(\langle\alpha\| - i\langle-\alpha\|)$	$e^{-i\frac{\pi}{2}(j^2-k^2)}\delta_{mj}\delta_{nk}$
Beam splitter ($\mathcal{E}_{BS}$)	$\|T\alpha_1 - R\alpha_2, R\alpha_1 + T\alpha_2\rangle$ $\times\langle T\alpha_1 - R\alpha_2, R\alpha_1 + T\alpha_2\|$	$\sqrt{\frac{m_1!m_2!n_1!n_2!}{j_1!j_2!k_1!k_2!}}\sum_{p=0}^{j_1}\sum_{q=0}^{k_1}(-1)^{j_1+k_1-p-q}$ $\times\binom{j_1}{p}\binom{j_2}{m_1-p}\binom{k_1}{q}\binom{k_2}{n_1-q}$ $\times T^{2p+2q+j_2+k_2-m_1-n_1}$ $\times R^{j_1+k_1+m_1+n_1-2p-2q}$ $\times\delta_{m_1+m_2,j_1+j_2}\delta_{n_1+n_2,k_1+k_2}$
Parametric down-conversion ($\mathcal{E}_{\text{PDC}}$)	$e^{r(\hat{a}_1\hat{a}_2-\hat{a}_1^\dagger\hat{a}_2^\dagger)}\|\alpha_1,\alpha_2\rangle$ $\times\langle\alpha_1,\alpha_2\|e^{r(\hat{a}_1^\dagger\hat{a}_2^\dagger-\hat{a}_1\hat{a}_2)}$	$\sqrt{\frac{m_1!m_2!n_1!n_2!}{j_1!j_2!k_1!k_2!}}$ $\times\frac{(\tanh r)^{m_1+n_1-j_1-k_1}}{(m_1-j_1)!\,(n_1-k_1)!\,(\cosh r)^{j_2+k_2-j_1-k_1+2}}$ $\times\,{}_2F_1\left(-j_1, m_2+1; m_1-j_1+1; \tanh^2 r\right)$ $\times\,{}_2F_1\left(-k_1, n_2+1; n_1-k_1+1; \tanh^2 r\right)$ $\times\,\delta_{m_2-m_1,j_2-j_1}\delta_{n_2-n_1,k_2-k_1}$

the hypergeometric function, $(x)_n := \Gamma(x+n)/\Gamma(x)$ the Pochhammer symbol and $\Gamma(\cdot)$ the Gamma function [62].

3.3 Conclusion

In this chapter, we have presented our new method for calculating the process tensor of an unknown quantum-optical process in the Fock basis(Equations (3.7) and (3.12)). This method eliminates P-function representation of input states and P-function regularization, which was necessary in Ref. [13]. Hence, we improved the original technique by removing the inherent ambiguity associated with P-function regularization (see Sec. 1.4).

We also have presented the multi-mode generalization of our method. This generalization is straightforward in comparison with that of Ref. [13], as in the latter the regularization functions for each mode are involved and the superoperator formula would be more complicated.

In Sec. 3.1.2, we have shown that, as the hybrid coherent-Fock representation is an entire function, knowing the effect of process on coherent states in the neighborhood of vacuum is sufficient to characterize the quantum process. Due to the entireness of this function, in principle, it is possible to characterize a quantum process by knowing its effects on the coherent states over any compact region of the phase space.

In Sec. 3.2, we have illustrated our method by analytically deriving corresponding superoperator operators of some fundamental quantum optical processes in the Fock basis. As the superoperator formula, in the Fock basis, proposed in Ref. [13] was based on using a regularized version of $P_{L,nm}(\alpha)$, the formula contains complicated integral. Hence, it was not possible to calculate the superoperators, which we have obtained analytically and derive the closed-form expressions by using Ref. [13].

As discussed in Sec. 1.4, coherent states are readily available in quantum optics; by having a simple mathematical framework and available probe states the task of QPT is quite feasible even for Hilbert spaces with large dimension. Hence, our new method provides a convenient way for complete characterization of any quantum-optical processes.

Chapter 4

Practical application

In this chapter, we develop a procedure for experimental application of our new method for the class of phase-invariant single-mode quantum optical processes. In an experiment, the first step towards QPT is preparing a set of known probe states $\{\rho_i\}$. Here coherent states, as the probe states, are available from a laser source, and the process output states are reconstructed by means of optical homodyne tomography.

In Sec. 4.1, we discuss the phase invariance symmetry of a quantum-optical process and derive the superoperator formula for phase-invariant processes. We introduce the procedure for calculating the superoperator in Sec. (4.2). In Sec. 4.3, we discuss the sources of the errors in our method and compare with those of the method in Ref. [13]. We conclude this chapter in the last section.

The results of my project presented in this chapter are as follows:

- the superoperator formula for phase-invariant processes,
- a procedure for calculation of the superoperator,
- a lower bound for the number of probe states.

4.1 Phase-invariant processes

Many practically relevant processes, including the single-mode processes studied in Sec. 3.2, exhibit phase invariance symmetry. The phase-invariant process is a process wherein for two input states identical up to an optical phase shift ϕ, the process outputs for these states differ by the same phase shift:

$$\mathcal{E}[e^{i\hat{n}\phi}\rho e^{-i\hat{n}\phi}] = e^{i\hat{n}\phi}\mathcal{E}(\rho)e^{-i\hat{n}\phi}, \tag{4.1}$$

where $e^{i\theta\hat{n}}$ is called the *phase-shifting* operator [25]. If the phase-shifting operator acts on a coherent state, it changes the phase of coherent state by ϕ:

$$e^{i\hat{n}\phi}|\alpha\rangle = |e^{i\phi}\alpha\rangle. \tag{4.2}$$

Hence, for such processes, it is convenient to express the probe coherent states in polar coordinates: $|\alpha\rangle = |re^{i\theta}\rangle = e^{i\hat{n}\theta}|r\rangle$.

The P-function of the operator $|m\rangle\langle n|$ (representation (3.3)) in polar coordinates is [41]

$$P_{mn}(r,\theta) = \frac{\sqrt{m!n!}}{(m+n)!} e^{r^2+i\theta(n-m)}(-1)^{m+n}\frac{\mathrm{d}^{m+n}}{\mathrm{d}r^{m+n}}\delta(r). \tag{4.3}$$

By inserting this form of P-function into Eq. (3.6) and performing integration by parts, we obtain the superoperator in polar coordinates

$$\mathcal{E}_{jk}^{mn} = \frac{\sqrt{m!n!}}{(m+n)!}\frac{\mathrm{d}^{m+n}}{\mathrm{d}r^{m+n}}\left[\int_0^{2\pi}\frac{\mathrm{d}\theta}{2\pi}e^{r^2+i\theta(n-m)}\langle j|\,\varrho_{\mathcal{E}}(r,\theta)\,|k\rangle\right]\Bigg|_{r=0}, \tag{4.4}$$

where

$$\varrho_{\mathcal{E}}(r,\theta) = \mathcal{E}\left(|re^{i\theta}\rangle\langle re^{i\theta}|\right). \tag{4.5}$$

For phase-invariant processes Eq. (4.1), we have

$$\begin{aligned}\langle j|\varrho_{\mathcal{E}}(r,\theta)|k\rangle &= \langle j|\,\mathcal{E}\left(e^{i\hat{n}\theta}|r\rangle\langle r|e^{-i\hat{n}\theta}\right)|k\rangle, \\ &= e^{i\theta(j-k)}\varrho_{\mathcal{E}}(r),\end{aligned} \tag{4.6}$$

with

$$\varrho_{\mathcal{E}}(r) = \langle j|\,\mathcal{E}\left(|r\rangle\langle r|\right)|k\rangle. \tag{4.7}$$

Using this property, the superoperator $\mathcal{E}$ (4.4) for phase-symmetric processes has the following explicit representation

$$\mathcal{E}_{jk}^{mn} = \frac{\sqrt{m!n!}}{(m+n)!}\frac{\mathrm{d}^{m+n}}{\mathrm{d}r^{m+n}}\left[e^{r^2}\langle j|\varrho_{\mathcal{E}}(r)|k\rangle\right]\Bigg|_{r=0}\delta_{m-j,n-k}, \tag{4.8}$$

where the Kronecker δ imposes $m-j=n-k$.

4.2 Calculating the superoperator

In this section, we introduce a procedure for calculating the superoperator of phase-invariant processes (4.8) from experimental data. In experimental tomography of phase-invariant processes [13, 42] it is sufficient to measure the process output for a discrete set of coherent states $\{|r_i e^{i\theta_0}\rangle\}_{i=1}^{L}$, with small values of r_i and the same phase, by using optical homodyne tomography (Sec. 1.2.1). As there is no preferred reference for phase, θ_0 can be set to zero. By representing the output states in the Fock basis, we have a set of matrices corresponding to the amplitude of the input coherent states $\{r_i, \langle j|\varrho_\varepsilon(r_i)|k\rangle\}_{i=1}^{L}$. Using these data points, one can fit a polynomial to corresponding set of matrix elements

$$g_{Q,jk}(r) = \sum_{l=0}^{Q} C_l(j,k) r^l, \tag{4.9}$$

where j and k denote the matrix element of the output state, $C_l(j,k)$ are coefficients of the polynomial, and Q is the degree of the polynomial (which depends on the dimension of the truncated Hilbert space). In order to achieve a good fitting, there is a lower bound on the required number of input coherent states L [64]

$$L \geq Q + 4. \tag{4.10}$$

The *index of determination* [64] of $g_{Q,jk}(r)$ is an indicator of good fit

$$R(g_{Q,jk}(r)) = \frac{\sum_{i=1}^{L}[g_{Q,jk}(r) - y]^2}{\sum_{i=1}^{L}[\langle j|\varrho_\varepsilon(r_i)|k\rangle - y]^2}, \tag{4.11}$$

where

$$y = \frac{1}{L}\sum_{i=1}^{L}\langle j|\varrho_\varepsilon(r_i)|k\rangle \tag{4.12}$$

and $0 \leq R(g_{Q,jk}(r)) \leq 1$. If $R(g_{Q,jk}(r)) \approx 1$ but $R(g_{Q-1,jk}(r))$ is not close to 1, one can say that the fitted polynomial is a good approximation of the actual function [64]

$$g_{Q,jk}(r) \approx \langle j|\varrho_\varepsilon(r)|k\rangle. \tag{4.13}$$

Furthermore, from Eq. (3.16) in polar coordinates and Eq. (4.7), we obtain

$$\langle j|\varrho_{\mathcal{E}}(r)|k\rangle = e^{-r^2}\sum_{n=0}^{\infty}\sum_{m=0}^{\infty}\frac{r^{n+m}}{\sqrt{n!m!}}\mathcal{E}_{jk}^{nm}. \tag{4.14}$$

From this equation, it follows that, for the phase-invariant processes [Eq. (4.8)], when $j-k$ is even or odd, $\langle j|\varrho_{\mathcal{E}}(r)|k\rangle$ and its analytic extension to negative values of r are even or odd functions of r, respectively. By taking into account the parity of this function, we have additional information to be used in the polynomial fitting procedure; the constructed polynomial has to contain only even or odd powers of r, respectively. Considering this property the inequality (4.10) becomes

$$L \geq \frac{Q+4}{2}; \tag{4.15}$$

hence the minimum number of input coherent states is decreased by a factor of two. In this way the precision of process estimation from the experimental data is substantially increased.

From the coefficients $C_l(j,k)$, Eq. (4.8) is further simplified to:

$$\begin{aligned}\mathcal{E}_{jk}^{mn} &= \frac{\sqrt{m!n!}}{(m+n)!}\frac{\mathrm{d}^{m+n}}{\mathrm{d}r^{m+n}}\left[\sum_{s=0}^{\infty}\frac{r^{2s}}{s!}\sum_{l=0}^{Q}C_l(j,k)r^l\right]\Bigg|_{r=0}\delta_{m-j,n-k}\\ &= \frac{\sqrt{m!n!}}{(m+n)!}\sum_{s=0}^{\infty}\sum_{l=0}^{Q}\frac{\delta_{m+n,2s+l}(m+n)!}{s!}C_l(j,k)\delta_{m-j,n-k}\\ &= \sqrt{m!n!}\sum_{s=0}^{\lfloor (m+n)\rfloor/2}\frac{C_{m+n-2s}(j,k)}{s!}\delta_{m-j,n-k}\,,\end{aligned} \tag{4.16}$$

where $\lfloor . \rfloor$ indicates the floor function. The last result is significant in that, through simple summation, one obtains the process tensor from the coefficients of the fitted polynomial using experimentally-reconstructed output states.

Moreover, if the dimension of the truncated Hilbert space is $d = N+1$, from Eq. (4.16) it follows that only terms of power $l \leq 2N$ of the fitted polynomial (4.9) contribute to the process tensor, so it is sufficient to use any $Q \geq 2N$. Hence, by using inequality (4.15), we obtain

$$L \geq N+2. \tag{4.17}$$

According to this inequality, we have a lower bound for the number of input coherent states required to calculate the process tensor over the Hilbert space with maximum number of N photons.

4.3 Sources of errors

In this section, we only discuss sources for the errors in the calculation of the process tensor from the experimental data. Assuming ideal coherent states are available in laboratory, there are three sources for the errors.

Due to finiteness of recourses, we consider the process estimation restricted to a finite-dimensional subset of $\mathscr{B}(\mathscr{H})$. This restriction is a source of error in characterizing the process tensor. For the specific example of a regularization operator (see Subsec. (2.3.1)), which restricts to the subspace with a fixed maximum number of N photons, we have shown an error bound on the estimation of the output states, for non-energy-increasing processes. The general method for finding the error bound for any quantum processes remains as an open question.

A second source of error in the calculation of the process tensor is due to the sampling of the process. In the above-mentioned method, we find the effect of an unknown quantum process on a discrete set of coherent states and then fit a polynomial function to the matrix elements of the output states. Hence, there is an error associated with polynomial fitting procedure.

Another source of error is due to the state tomography of the output states. As discussed Sec. 1.2, to reconstruct the process output state from the experimental data many copies of each probe states are required, and many measurements must be performed. Due to finiteness of resource (number of multiple copies and measurement, and time) there is always an error associated with the QST.

Considering the last two errors, there is an uncertainty associated with each elements of the process tensor $\Delta\mathcal{E}_{jk}^{mn}$, which are calculated by our procedure. The method for estimating

$$\mathcal{E}_{jj}^{nn} \pm \Delta\mathcal{E}_{jj}^{nn} = \left(\begin{array}{cccc|c} \mathcal{E}_{00}^{00} \pm \Delta\mathcal{E}_{00}^{00} & \mathcal{E}_{00}^{11} \pm \Delta\mathcal{E}_{00}^{11} & \cdots & \mathcal{E}_{00}^{NN} \pm \Delta\mathcal{E}_{00}^{NN} & \vdots \\ \mathcal{E}_{11}^{00} \pm \Delta\mathcal{E}_{11}^{00} & \mathcal{E}_{11}^{11} \pm \Delta\mathcal{E}_{11}^{11} & \cdots & \mathcal{E}_{11}^{NN} \pm \Delta\mathcal{E}_{11}^{NN} & \vdots \\ \vdots & \vdots & \cdots & \vdots & \vdots \\ \vdots & \vdots & \cdots & \vdots & \vdots \\ \vdots & \vdots & \cdots & \vdots & \vdots \\ \mathcal{E}_{NN}^{00} \pm \Delta\mathcal{E}_{NN}^{00} & \mathcal{E}_{NN}^{11} \pm \Delta\mathcal{E}_{NN}^{11} & \cdots & \mathcal{E}_{NN}^{NN} \pm \Delta\mathcal{E}_{NN}^{NN} & \vdots \\ \hline \vdots & \vdots & \cdots & \vdots & \vdots \\ \vdots & \vdots & \cdots & \vdots & \vdots \end{array}\right) \begin{array}{l} \left.\vphantom{\begin{array}{c}a\\a\\a\\a\\a\end{array}}\right\} N+1 \\ \\ \end{array}$$
$$\underbrace{\qquad\qquad\qquad\qquad}_{N+1}$$

Figure 4.1: As the superoperator is a rank-4 tensor, the errors are shown for diagonal elements. There are two kinds of errors: the errors associated with state tomography and interpolation $\Delta\mathcal{E}_{jj}^{nn}$, and the error associated with projection to the subspace with maximum N number of photons.

an upper bound on this uncertainty is a future work. The first error is different in that it does not contribute to the uncertainty of the process tensor elements; this error is due to ignoring high-energy behavior of the process (see Fig. 4.1).

In the original proposal for csQPT [13], beside these sources of errors, there is another source of error associated with the P-function regularization. Note that this error is an inherent error in the process tomography method, which we eliminate by improving the method.

4.4 Conclusion

In this chapter, we have presented a practical procedure for calculating the process tensor from the experimental data for the phase-symmetric processes. In Sec. 4.1, we obtained the superoperator formula [Eq. (4.8)] for the phase-symmetric processes, where only depends on the amplitude of input coherent states. Then, in Sec. 4.2, we presented a procedure for solving Eq. (4.8) from the experimental data. We showed that by finding effects of a quantum process on a discrete set of coherent states around the vacuum and exploiting the symmetry or antisymmetry of the function $\langle j|\varrho_\varepsilon(r)|k\rangle$, one can construct a polynomial that is a good approximation

of the actual function , and use this polynomial to calculate the superoperator (4.16). Moreover, we found a lower bound for the required number of coherent states as the probe states (4.17). In Sec. 4.3, we discussed the sources of the errors in our method and compared it with those of Ref. [13]. We showed that, apart from the error associated with the truncation of the Hilbert space, there are two other sources of errors due to QST and polynomial fitting, while there is an additional source of error associated with the P-function regularization in the original proposal [13].

Chapter 5

Conclusions

In this chapter, we review the main results of this study. The main goal of this thesis has been to introduce a more efficient method for complete quantum-optical process tomography.

The following section summarizes the main achievements of my M.Sc. project, which are presented in this thesis. The last section suggests some future works based on this study.

5.1 Results

As discussed in Chapter 1, coherent states are easily generated probe states for tomography of unknown quantum-optical processes; hence, coherent-state process tomography is a convenient method with available probe states for characterizing unknown quantum optical processes. In this study (Chap. 3 and Chap. 4), we have presented a new, more efficient data processing technique [14] for estimating a quantum process from an experimental procedure similar to that of Ref. [13] in the Fock basis. Using this technique one can characterize any complex processes in quantum optics, which may be used in quantum information processing and communication. Here we summarize the advantages of our new method.

As discussed in Sec. 1.4, the original formulation was based on regularization and filtering of the Glauber-Sudarshan representations for quantum states, which are cumbersome to implement numerically. Furthermore, Ref. [13] introduces additional errors associated with regularization of the P-function (see Sec. 4.3). In contrast, our new method to determine the process superoperator [Chap. 3, Eq. (3.7) or Eq. (3.12)] is mathematically simpler, computationally faster and unique up to the choice of the energy cutoff.

Moreover, we presented straightforward generalizations of coherent state quantum process

tomography to multi-mode in Subsec. 3.1.1. Although the method in Ref. [13] was also generalizable to the M-mode case, as each mode of electromagnetic field should be regularized, and there are M parameters need to be defined, the resultant formula for the superoperator would be too complicated. We also discussed the generalization of this method to non-trace-preserving conditional processes [3.1].

In Sec. 3.2, we have illustrated the new framework through several examples. We have shown that it is straightforward to derive an analytically exact and unique closed-form expressions for the superoperators for quantum-optical processes whose effect on coherent states is known, while by using Ref. [13] this could be only done numerically.

An interesting consequence implied by our formulation [in particular, Eqs. (3.7) and (3.12)] is that complete information about a quantum-optical process is entirely captured by its effect on a compact set of all coherent states $|\alpha\rangle$ in the immediate vicinity of the vacuum state. As discussed in Subsec. 3.1.2, this is due to the entireness property of the image of processes on coherent states. It thus appears sufficient to perform tomography experiments only for a range of coherent states whose mean photon number is much smaller than that required for the method of Ref. [13].

In Chap. 4, we presented a procedure for calculating the superoperator of phase-invariant processes. We showed that the formula to find the superoperator reduces to a simple summation of coefficients of a polynomial fitted to the matrix elements of the experimentally reconstructed output states. We also found that the lower bound for the required number of coherent states as probe states is $\dim \widetilde{\mathscr{H}} + 1$.

For the time being, we have provided an evaluation of the error in the process estimation associated with the use of the regularization operator introduced in Sec. 2.3, in the Fock basis. For the class of processes respecting a certain energy constraint (which includes all processes that do not amplify the energy), we have determined (i) the cutoff dimension that is sufficient in order to achieve a certain degree of approximation accuracy, as well as (ii) the upper bound

on the error of estimation for a given cutoff dimension. We have shown that the accuracy of process estimation scales inversely with the square root of the photon-number cutoff.

5.2 Future work

In this section, we suggest two future works based on our new method.

As discussed in Subsec. 3.1.2, a quantum process can be characterized by knowing its effect on low-amplitude coherent states around the origin in the phase space. This is due to the entireness property of the hybrid coherent-Fock state representation $\langle j|\mathcal{E}(|\alpha\rangle\langle\alpha|)|k\rangle$, which has to be reconstructed from the experimental data. Therefore, in principle, it must be possible to characterize a quantum process by finding its effect on a set of coherent states in any compact region of the phase space. Considering this fact, one can find a formulation for the superoperator by which a quantum process can be characterized by knowing the effect of the process on coherent states around any point α_0 in the phase space.

In this thesis, we have presented an experimental procedure for calculating the superoperator for phase-invariant processes. This procedure can be easily generalized to any processes by fitting two-dimensional polynomials to the matrix elements of the output states for a set of coherent states as input states. Also, as discussed in Subsec. 3.1.2, to characterize a quantum process only the effects of the process on the coherent states within distance ε from the vacuum state are required. In principle, there must be a relation between ε and the dimension of subspace of the Hilbert space to which process tomography is restricted. This relation remains as an open question.

Bibliography

[1] M. A. Nielsen and I. L. Chuang, *Quantum computation and quantum information* (Cambridge University Press, Cambridge, UK, 2000).

[2] M. Paris and J. Řeháček, Eds., *Quantum state estimation*, Lecture Notes in Physics Vol. **649** (Springer, Berlin, 2004).

[3] M. Mohseni, A. T. Rezakhani, and D. A. Lidar, *Quantum-process tomography: Resource analysis of different strategies*, Phys. Rev. A **77**, 032322 (2008).

[4] I. L. Chuang and M. A. Nielsen, *Prescription for experimental determination of the dynamics of a quantum black box*, J. Mod. Opt. **44**, 2455 (1997).

[5] J. F. Poyatos, J. I. Cirac, and P. Zoller, *Complete characterization of a quantum process: the two-bit quantum gate*, Phys. Rev. Lett. **78**, 390 (1997).

[6] G. M. D'Ariano and L. Maccone, *Measuring quantum optical Hamiltonians*, Phys. Rev. Lett. **80**, 5465 (1998).

[7] A. Luis and L. L. Sánchez-Soto, *Measuring quantum input-output processes: phase-space representation of transformations*, Phys. Lett. A **261**, 12 (1999).

[8] R. Gutzeit, S. Wallentowitz, and W. Vogel, *Reconstructing the time evolution of a quantized oscillator*, Phys. Rev. A 61, 062105 (2000).

[9] G. M. D'Ariano and P. Lo Presti, *Quantum tomography for measuring experimentally the matrix elements of an arbitrary quantum operation*, Phys. Rev. Lett. **86**, 4195 (2001).

[10] D. G. Fischer, H. Mack, M. A. Cirone, and M. Freyberger, *Enhanced estimation of a noisy quantum channel using entanglement*, Phys. Rev. A **64**, 022309 (2001).

[11] M. F. Sacchi, *Maximum-likelihood reconstruction of completely positive maps*, Phys. Rev. A **63**, 054104 (2001).

[12] P. Kok, W. J. Munro, K. Nemoto, T. C. Ralph, J. P. Dowling, and G. J. Milburn, *Linear optical quantum computing with photonic qubits*, Rev. Mod. Phys. **79**, 135 (2007).

[13] M. Lobino, D. Korystov, C. Kupchak, E. Figueroa, B. C. Sanders, and A. I. Lvovsky, *Complete characterization of quantum-optical processes*, Science **322**, 563 (2008).

[14] S. Rahimi-Keshari, A. Scherer, A. Mann, A. T. Rezakhani, A. I. Lvovsky, and B. C. Sanders, *Quantum process tomography with coherent states*, submitted to New Journal of Physics. http://arxiv.org/abs/1009.3307

[15] K. Kraus, *States, effects and operations* (Springer, Berlin, 1983).

[16] W. Heisenberg, *The physical principles of the quantum theory* (Univ. Chicago Pres, Dover, NY, 1930).

[17] J. von Neumann, *Mathematical foundations of quantum mechanics* (Princeton Univ. Press, NJ, 1955).

[18] W. K. Wootters and W.H. Zurek, *A single quantum cannot be cloned*, Nature **299**, 802 (1982).

[19] G. M. D'Ariano, M. G. A. Paris, and M. F. Sacchi, in *Quantum state estimation*, M. Paris and J. Řeháček, Eds, Lecture Notes in Physics **649** (Springer, Berlin, 2004).

[20] U. Fano, *Description of states in quantum mechanics by density matrix and operator techniques*, Rev. Mod. Phys. 29, 74 (1957).

[21] R. Blume-Kohout, *Optimal, reliable estimation of quantum states* , New J. Phys. **12**, 043034 (2010).

[22] A. I. Lvovsky and M. G. Raymer, *Continuous-variable optical quantum-state tomography*, Rev. Mod. Phys. **81**, 299 (2009).

[23] H. P. Yuen and V. W. S. Chan, *Noise in homodyne and heterodyne detection*, Opt. Lett. **8**, 177 (1983).

[24] G. L. Abbas, V. W. S. Chan, and S. T. Yee, *Local-oscillator excess-noise suppression for homodyne and heterodyne detection*, Opt. Lett. **8**, 419 (1983).

[25] U. Leonhardt, *Measuring the quantum state of light* (Cambridge Univ. Press, Cambridge, 1997).

[26] J. B. Altepeter, D. Branning, E. Jeffrey, T. C. Wei, P. G. Kwiat, R. T. Thew, J. L. OBrien, M. A. Nielsen, and A. G. White, *Ancilla-assisted quantum process tomography*, Phys. Rev. Lett. 90, 193601 (2003).

[27] F. De Martini, A. Mazzei, M. Ricci, and G. M. D'Ariano, *Exploiting quantum parallelism of entanglement for a complete experimental quantum characterization of a single-qubit device*, Phys. Rev. A 67, 062307 (2003).

[28] G. M. D'Ariano and P. Lo Presti, *Imprinting complete information about a quantum channel on its output state*, Phys. Rev. Lett. 91, 047902 (2003).

[29] M. Mohseni and D. A. Lidar, *Direct characterization of quantum dynamics*, Phys. Rev. Lett. 97, 170501 (2006).

[30] M. Mohseni and D. A. Lidar, *Direct characterization of quantum dynamics: General theory*, Phys. Rev. A 75, 062331 (2007).

[31] M. A. Nielsen, E. Knill, and R. Laflamme, *Complete quantum teleportation using nuclear magnetic resonance*, Nature 396, 52 (1998).

[32] A. M. Childs, I. L. Chuang, and D. W. Lueng, *Realization of quantum process tomography in NMR*, Phys. Rev. A **64**, 012314 (2001).

[33] N. Boulant, T. F. Havel, M. A. Pravia, and D. G. Cory, *Robust method for estimating the Lindblad operators of a dissipative quantum process from measurements of the density operator at multiple time points*, Phys. Rev. A **67**, 042322 (2003).

[34] S. H. Myrskog, J. K. Fox, M. W. Mitchell, and A. M. Steinberg, *Quantum process tomography on vibrational states of atoms in an optical lattice*, Phys. Rev. A **72**, 013615 (2005).

[35] M. Howard, J. Twamley, C. Wittmann, T. Gaebel, F. Jelezko, and J Wrachtrup, *Quantum process tomography and Linblad estimation of a solid-state qubit*, New J. Phys. **8**, 33 (2006).

[36] J. L. O'Brien, G. J. Pryde, A. Gilchrist, D. F. V. James, N. K. Langford, T. C. Ralph, and A. G. White, *Quantum process tomography of a controlled-NOT gate*, Phys. Rev. Lett. **93**, 080502 (2004).

[37] M. W. Mitchell, C. W. Ellenor, S. Schneider, and A. M. Steinberg, *Diagnosis, prescription, and prognosis of a Bell-state filter by quantum process tomography*, Phys. Rev. Lett. **91**, 120402 (2003).

[38] T. M. Graham, P. G. Kwiat, and J. Barreiro, *Quantum process tomography by direct characterization of quantum dynamics using hyperentangled photons* in Conference on Lasers and Electro-Optics, OSA Technical Digest (CD) (Optical Society of America, 2010), paper JThC2.

[39] L. Mandel and E. Wolf, *Optical coherence and quantum optics* (Cambridge University Press, Cambridge, 1995).

[40] R. J. Glauber, *Photon correlations*, Phys. Rev. Lett. **10**, 84 (1963).

[41] E. C. G. Sudarshan, *Equivalence of semiclassical and quantum mechanical descriptions of statistical light beams*, Phys. Rev. Lett. **10**, 277 (1963).

[42] M. Lobino, C. Kupchak, E. Figueroa, and A. I. Lvovsky, *Memory for light as a quantum process*, Phys. Rev. Lett. 102, 203601 (2009).

[43] K. E. Cahill, *Coherent-state representations for the photon density operator*, Phys. Rev. **138**, B1566 (1965).

[44] K. E. Cahill, *Pure states and the P representation*, Phys. Rev. **180**, 1239 (1969).

[45] K. E. Cahill, *Regularization of the P representation*, Phys. Rev. **180**, 1244 (1969).

[46] N. Chandra and R. Prakash, *Regularized P representation*, Phys. Rev. D 7, 1936 (1973).

[47] J. R. Klauder, *Improved version of optical equivalence theorem*, Phys. Rev. Lett. **16**, 534 (1966).

[48] I. M. Gel'fand and G. E. Shilov, *Generalized functions*, Vol. 1 (Academic Press, New York, 1964).

[49] E. Knill, R. Laflamme, and G. J. Milburn, *A scheme for efficient quantum computation with linear optics*, Nature 409, 46 (2001).

[50] A. Yu. Kitaev, *Quantum computations: algorithms and error correction*, Russ. Math. Surv. **52**, 1191 (1997).

[51] G. M. D'Ariano, D. Kretschmann, D. Schlingemann, and R. F. Werner, *Reexamination of quantum bit commitment: The possible and the impossible*, Phys. Rev. A **76**, 032328 (2007).

[52] M. Reed and B. Simon, *Methods of modern mathematical physics, Vol. 1: Functional analysis* (Academic Press, New York, 1980).

[53] L. Schwartz, *Théorie des distributions*, Vol. 1 (Hermann et Cie., Paris, 1951).

[54] K. E. Cahill and R. J. Glauber, *Density operators and quasiprobability distributions*, Phys. Rev. **177**, 1882 (1969).

[55] J. F. Scherson, H. Krauter, R. K. Olsson, B. Julsgaard, K. Hammerer, I. Cirac, and E. S. Polzik, *Quantum teleportation between light and matter*, Nature **443**, 557 (2006).

[56] D. Kretschmann, D. Schlingemann, and R. F. Werner, *The information-disturbance tradeoff and the continuity of Stinespring's representation*, IEEE Trans. Inf. Theory **54**, 1708 (2008).

[57] A. Ourjoumtsev, R. Tualle-Brouri, J. Laurat, and P. Grangier, *Generating optical Schrödinger kittens for quantum information processing*, Science **312**, 83 (2006).

[58] A. Zavatta, S. Viciani, and M. Bellini, *Quantum-to-classical transition with single-photonadded coherent states of light*, Science **306**, 660 (2004).

[59] G. J. Milburn, *Quantum and classical Liouville dynamics of the anharmonic oscillator*, Phys. Rev. A **33**, 674 (1986).

[60] B. Yurke and D. Stoler, *Generating quantum mechanical superpositions of macroscopically distinguishable states via amplitude dispersion*, Phys. Rev. Lett. **57**, 13 (1986).

[61] B. Yurke, S. L. McCall, and J. R. Klauder, *SU(2) and SU(1,1) interferometers*, Phys. Rev. A **33**, 4033 (1986).

[62] M. Abramowitz and I. A. Stegun, *Handbook of mathematical functions* (Dover, New York, 1972).

[63] C. Gerry and P. L. Knight, *Introductory quantum optics* (Cambridge University Press, New York, 2005).

[64] M. J. Maron, *Numerical analysis: A practical approach* (Macmillan, New York, 1987).